HIPPOCAMPUS 18:879–898 (2008)

Inverse Relationship Between Adult Hippocampal Cell Proliferation and Synaptic Rewiring in the Dentate Gyrus

Markus Butz,[1]* Gertraud Teuchert-Noodt,[2] Keren Grafen,[3] and Arjen van Ooyen[4]

ABSTRACT: Adult neurogenesis is a key feature of the hippocampal dentate gyrus (DG). Neurogenesis is accompanied by synaptogenesis as new cells become integrated into the circuitry of the hippocampus. However, little is known to what extent the embedding of new neurons rewires the pre-existing network. Here we investigate synaptic rewiring in the DG of gerbils (*Meriones unguiculatus*) under different rates of adult cell proliferation caused by different rearing conditions as well as juvenile methamphetamine treatment. Surprisingly, we found that an increased cell proliferation reduced the amount of synaptic rewiring. To help explain this unexpected finding, we developed a novel model of dentate network formation incorporating neurogenesis and activity-dependent synapse formation and remodelling. In the model, we show that homeostasis of neuronal activity can account for the inverse relationship between cell proliferation and synaptic rewiring. © **2008 Wiley-Liss, Inc.**

KEY WORDS: hippocampus; neurogenesis; structural plasticity; homoeostasis; neural network model

INTRODUCTION

Cell proliferation (CP) of neuronal precursor cells (Kaplan and Bell, 1983, 1984) add new neurons to the adult hippocampal DG in higher mammals (Altman and Das, 1965; Gould and Gross, 2002; reviewed in Ming and Song, 2005) and humans (Eriksson et al., 1998). A fraction of these new neurons is persistent and develops into functional granule cells (Van Praag et al., 2002; Kempermann et al., 2004), contributing to adult neurogenesis. The key to understanding the functional meaning of young neurons in mature neuronal networks is the timing of their synaptic integration (Aimone et al., 2006). Synaptic integration in general means the capability to induce long-term potentian [long-term potentiation (LTP)], as recently observed in young granule cells (Schmidt-Hieber et al., 2004; Ge et al., 2007b; Tashiro et al., 2007) and analyzed by a variety of computational models (Cecchi, 2001; Shors et al., 2001; reviewed in Gazzaniga et al., 2002; Chambers et al., 2004; Crick and Miranker, 2006; Wiskott et al., 2006). However, the discussion on the functional meaning of hippocampal neurogenesis (Becker, 2005) should also include the preceding structural process of synapse formation (Toni et al., 2007) and network rewiring.

Progenitor cells (Kaplan and Bell, 1983, 1984) migrate from the germinative zone in the subgranular into the granular layer (Schlessinger et al., 1975; Rickmann et al., 1987) and initially form transient synapses (Stanfield and Trice, 1988; Markakis and Gage, 1999) and extend their axons to the hippocampal CA3 region (Hastings and Gould, 1999). After 2 wks, young granule cells express the first dendritic spines and continue remodelling their synaptic connectivity for at least 2 month after mitosis (Laplagne et al., 2006; Piatti et al., 2006; Zhao et al., 2006; Ge et al., 2007b; Tashiro et al., 2007; Toni et al., 2007). Differentiating dendrites first perturb the inner molecular layer (Kaplan and Bell, 1983; Cameron et al., 1993; Seki and Arai, 1993) and express neurotrophic factors (Cameron et al., 1993; Seki and Arai, 1993). Thereby, young granule cells compete with adjacent cells for presynaptic contacts, as their survival highly depends on pre- and postsynaptic support (Linden, 1994) as well as on balanced levels of excitation and inhibition (Lehmann et al., 2005; Meltzer et al., 2005). This raises the interesting question to what extent young neurons can induce structural plasticity in pre-existing dentate networks.

In order to investigate the relationship between synaptic rewiring and CP in the adult DG, we used young adult gerbils (*Meriones unguiculatus*). Gerbils are an ideal animal model because they show a pronounced synaptic rewiring under normal control conditions (Keller et al., 2000). For control conditions, animals were reared under (semi-) natural conditions (NRC), which lead to normal behavioral and brain development (Winterfeld et al., 1998). In contrast, gerbils kept under isolated and impoverished rearing conditions (IRC) after weaning, develop anxiety and stereotypic behaviors (Winterfeld et al., 1998). Anatomically, young adult gerbils (postnatal day 90, p90) from the latter group show a significantly reduced meso-prefrontal dopamine projection (Winterfeld et al., 1998; Neddens et al., 2001). Remarkably, synaptic rewiring in the DG of these animals is strongly

[1] **Bernstein Center for Computational Neuroscience Göttingen, Max-Planck-Institut for Dynamics and Selforganization, Bunsenstr. 10, Göttingen, Germany;** [2] **Department for Neuroanatomy, University of Bielefeld, Bielefeld, Germany;** [3] **Department for Cognitive Neurobiology, University of Bielefeld, Bielefeld, Germany;** [4] **Department of Experimental Neurophysiology, Center for Neurogenomics and Cognitive Research, VU University Amsterdam, De Boelelaan 1085, HV Amsterdam, The Netherlands**

Additional Supporting Information may be found in the online version of this article.

*Correspondence to: Dr. Markus Butz, Bernstein Center for Computational Neuroscience Göttingen, Max-Planck-Institut for Dynamics and Selforganization, Bunsenstr. 10, 37073 Göttingen, Germany.
E-mail: mbutz@bccn-goettingen.de

Accepted for publication 19 March 2008
DOI 10.1002/hipo.20445
Published online 14 May 2008 in Wiley InterScience (www.interscience.wiley.com).

reduced (Keller et al., 2000), while CP is significantly increased (BrdU staining: Hildebrandt, 1999; Hildebrandt et al., 1999; Keller et al., 2000). If this inverse relation between synaptic rewiring and CP holds true, we expect that down-regulating CP rates in isolated-reared animals will lead to stronger synaptic remodelling. From former studies with gerbils we know that CP rates respond to pharmacological interventions (Dawirs et al., 1998; reviewed in Lehmann et al., 2005). In particular, methamphetamine acutely suppresses CP in adult animals (Teuchert-Noodt et al., 2000) as well as after single juvenile treatment (Hildebrandt et al., 1999). Thus, in this study we treated young gerbils (p14) with a single high dose of methamphetamine obtaining normal CP rates at p90 even under isolated rearing conditions. In former studies (Hildebrandt et al., 1999), the CP rate suppressing effect of methamphetamine was present in both hemispheres but always lateralized to the left hemisphere, which is why we investigated synaptic rewiring in both hemispheres. As predicted, synaptic rewiring in the DG of methamphetamine-treated, isolated-reared animals was increased in both hemispheres at p90 but only significant in the left hemisphere.

We used a novel neuronal network model (Butz, 2006; Butz et al., 2006) to try and explain this counterintuitive, inverse relationship between CP and synaptic rewiring. Our model implements the structural processes of neurogenesis, synapse formation and synaptic rewiring. It is the first model that allows the investigation of both synaptic and cellular turnover in an interdependent manner. The aim of the modeling was not to produce an a priori defined behavior but was rather used in a bottom-up manner to study the consequences of the interplay between neurogenesis, synapse formation, and neuronal activity. In the model, axonal terminals and dendritic spines develop in an activity-dependent fashion and form synapses by merging postsynaptic dendritic spines and presynaptic axonal terminals. Importantly, neurons adapt their synaptic connectivity so as to keep their average firing rates at a constant level (homeostasis; cp. (Wolff and Wagner, 1983; Dammasch et al., 1986; Van Ooyen and Van Pelt, 1994; Van Ooyen et al., 1995; Chechik et al., 1999). The results of our modeling study suggest that this homeostatic structural plasticity can account for the observed relation between CP and synaptic turnover.

MATERIALS AND METHODS

Experimental Approach

Synaptic rewiring is carried by autophagic degradation of remodeling axon terminals, as we have shown for young adult (postnatal day 90) gerbils (Dawirs et al., 1992; Keller et al., 2000) and for other species (*see below*). In the process of autophagic degradation, transient lysosomal accumulations (LAs), multivesicular bodies and other decomposing organelles appear within the degrading presynaptic terminal. In rat visual cortex, autophagic degradation was observed after undercutting the visual cortex leaving horizontal connections intact (Holzgraefe et al., 1981). Secondary LAs periodically appeared weeks and months after the lesion, which could therefore not be attributed to a primary autophagic degradation and degeneration of fiber terminals that occurs up to 5 days after the lesion; these secondary LAs were proposed to arise from a late compensatory synaptic rewiring. LAs were found also during postnatal development (Wolff et al., 1989) and for different regions of the intact brain of adult rats (Leutgeb, 1986). These regions include the stratum lucidum in the hippocampus, the habenular nuclei and the glomerula of the olfactory bulb.

In order to quantify LAs in degrading axonal terminals by light microscopy, a silver impregnation of LAs was developed (Gallyas et al., 1980). The electron microscopic (EM) and ultrathin section analysis of the so-prepared material showed that the silver stained LAs were, in fact, located in remodeling axonal terminals (Teuchert-Noodt et al., 1991; Dawirs et al., 2000) and coincided during development with the period of the highest synapse formation (Wolff et al., 1989) as measured according to Nixdorf (Nixdorf, 1986; Nixdorf and Bischof, 1986). Thus, the Gallyas-staining can be taken as a suitable method for indicating periods of pronounced synaptic rewiring (cp. Wolff et al., 1989). Moreover, LAs differ in form and size from larger and coarse lysosomes in glia cells. Using Gallyas-staining, partly combined with EM, revealed LA in a variety of brain systems of higher vertebrates (mammalian iso- and archicortex: Wolff et al., 1989; Wolff and Missler, 1992; avian sensory, motor and associative systems: Teuchert-Noodt et al., 1991; cerebellum of the mallard (*Anas Platyrhynchos*) and Peking ducks (*Forma domestica*): Teuchert-Noodt and Dawirs, 1996; hippocampal DG of mice (*Acomys cahirhinus*): Dawirs et al., 1992; gerbils (*Meriones unguiculatus*): Dawirs et al., 2000; Keller et al., 2000). In addition, the silver staining technique is suitable for quantifying LA in the DG of gerbils over life time (Dawirs et al., 2000; Keller et al., 2000), showing an initial postnatal increase in the inner molecular layer, a stable state throughout adulthood, and an increasing general degeneration of synapses in aged animals.

Considering all this, Gallyas staining was the first technique (before time lapse imaging by confocal microscopy was available) that made it possible to show the dynamics of synaptic and, in particular, axonal remodeling. Standard synapse markers such as synaptophysin are not suitable for estimating rewiring because it merely gives total synapse densities.

Design of study

We used a total of 24 male gerbils (*Meriones unguiculatus*) for light microscopy quantification of LA patterns by the Gallyas-staining technique for both hemispheres. Animals from the first of three groups were kept under (semi-) natural rearing conditions (NRC), meaning that, after weaning, they were reared in a social group and were housed in large cages ($1 \times 1\ m^2$) with tubes and boxes to hide in and wooden branches to play with. The individuals from a second group were, after weaning, reared under isolated and impoverished conditions (IRC) in standard Macrolon cages sized 30 cm × 40 cm. Both groups were treated with saline intraperitoneal (i.p.) on post-

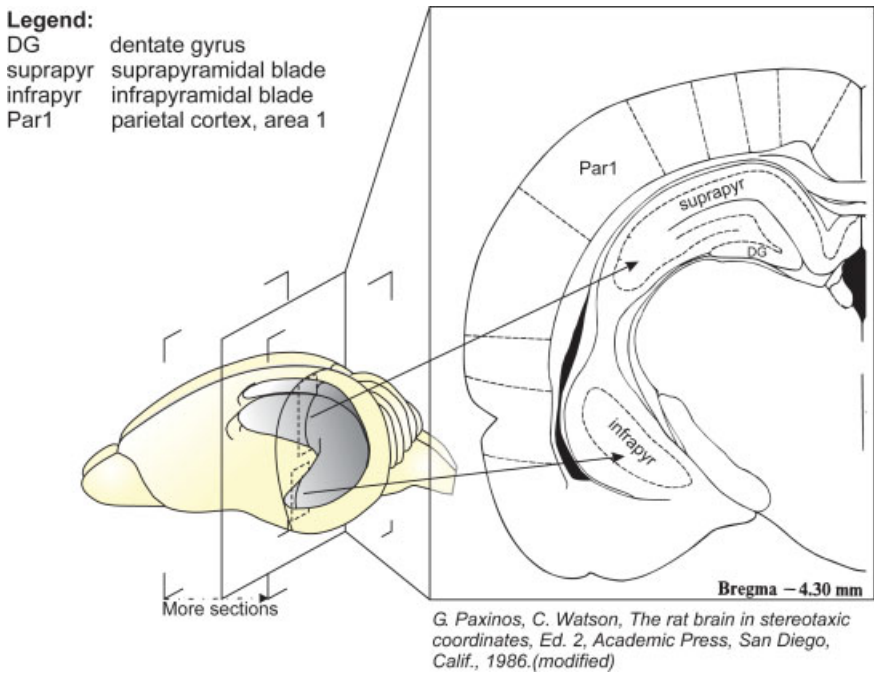

FIGURE 1. Hippocampal sections. Three-dimensional position of the hippocampal formation in the rodent brain. Frontal sections were taken for staining and light microscopy assessment. See further main text. [Color figure can be viewed in the online issue, which is available at www.interscience.wiley.com.]

natal day 14 (p14). In a third group, animals from the isolated rearing conditions were additionally treated with a single dose of methamphetamine (MA, Sigma, M-8,750) i.p. on p14 (IRC/MA). On postnatal day 90 (p90), 8 left (*l*) and 6 right (*r*) hemispheres from NRC animals, 7 *l* (5 *r*) from IRC animals and 7 *l* (8 *r*) from IRC/MA animals were successfully stained and quantified. All animals were kept under normal day/night cycles. Food and water were provided ad libidum.

Silver staining of lysosomal accumulations (LA)

Animals were transcardially perfused under deep ether anesthesia with 5% formalin. The brains were subsequently kept in formalin for 2 wks at 4°C. The frozen brains were cut in 80 μm thin frontal slices. Every second slice from the septal pole of the hippocampus to the temporal pole was used for staining (Fig. 1). In total, at least five sections from each brain were taken. According to the procedure described by Gallyas et al. (1980), the floating slices were prepared in an alkalinic acid (pH 13) containing 9% sodium hydroxide and 1% ammonium nitrate and subsequently silver impregnated by a silver nitrate solution containing 9% sodium hydroxide, 16% ammonium nitrate and 50% silver nitrate. The optimum silver concentration was estimated by examining stained test-slices by light microscopy. After impregnation, the slices were washed three times in changing washing solutions (solution: 30% ethyl-alcohol with 0.5 g sodium carbonate mixed with 1% ammonium nitrate). The developer contained 15 ml 40% formalin and 0.5% citric acid in 1,000 ml 10% ethyl alcohol. After another washing, the slices were air-dried, mounted on slides and embedded in DPX.

Computerized assessment of silver granules

The prepared sections were viewed in dark field at 125× magnification with a light microscope (Polyvar, Reichert-Jung). Pictures were taken of the DG and the parietal cortex (PC) by a digital camera (ProgRes 3008mF, Jenoptik, Jena). We developed a classification algorithm implemented in MATLAB Vers. 6 in order to count the number of LAs automatically. The classification algorithm (Fig. 2a) consists of four steps basically using linear filtering techniques and a threshold operator to distinguish light silver grains from a dark background (see Fig. 6a). In the first step, the digital image of one measuring field was transferred to an intensity gray scale image and, secondly, normalized by setting its median value to zero level (negative values were set to zero). In the third step, a linear filter with a 3 × 3-filtering matrix M was applied to the image:

$$M := \begin{pmatrix} -0.2 & -0.05 & -0.2 \\ -0.05 & 1 & -0.05 \\ -0.2 & -0.05 & -0.2 \end{pmatrix}, \quad \text{with} \sum_{i,j} x_{i,j} = 0$$

This method enhanced the contrast between a few-pixels sized, bright silver granules and the dark background. A threshold separates the classification between silver granules and background. In

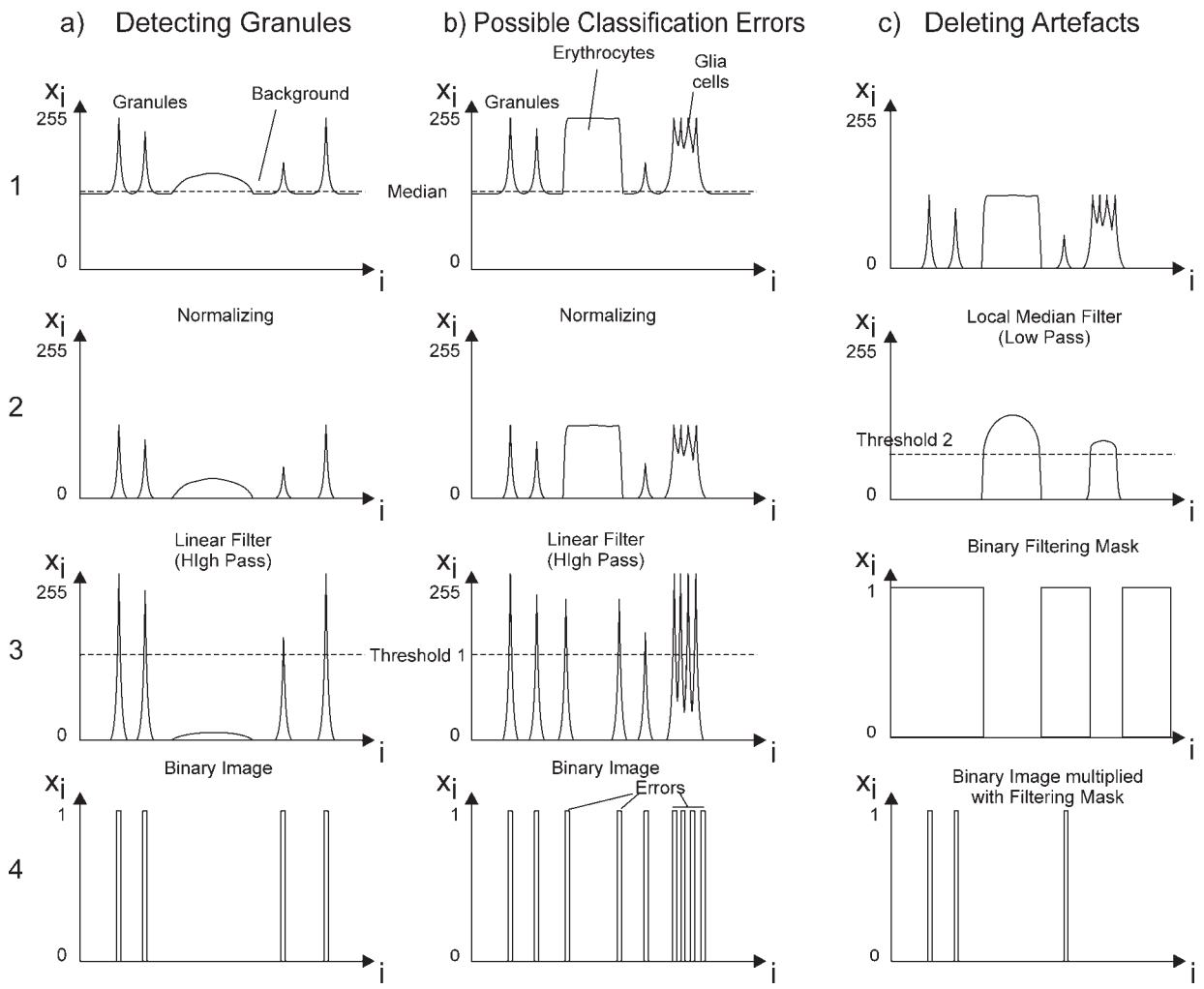

FIGURE 2. Automatic assessment of Gallyas staining. (a) Detecting LAs by applying linear filtering. For this purpose, the digital microscopy image is converted into a gray-scale image (1), normalized to its median (2) and filtered by a local linear high-pass filter (3). White spots in the obtained black-and-white image, indicating detected LAs, are thinned out to a single pixel (4) in order to be counted. (b) Local high-pass filtering leads to classification errors when applied to extended or diffuse light regions in the image arising from staining artifacts. (c) To remove classification errors, a local median filtering is subsequently applied to mark regions in the image where the local median is higher than the background. LAs counted in these regions are deleted.

the fourth step, white spots of detected silver granules in the black-and-white image were thinned out to a single pixel in order to count the number of the granules irrespective of their size. These steps are repeated for all measuring fields.

Detecting and erasing staining artifacts

As Figure 2b shows, classification errors arise from high-pass filtering strongly stained large or heterogeneous structures such as erythrocytes or lysosomal processes in glia cells, respectively. Thus, after classification we use a second filtering procedure (Fig. 2c) to clean the image from artifacts in the staining. These artifacts can be distinguished from the background by applying a local median filter to the normalized image (taken from Step 2 in Fig. 2b). In order to erase false positive classifications from the image, we define a filter mask on the basis of the local median filtering. The filtering mask is obtained by setting all local median values that are above a second threshold to zero and every other value to one. Subsequently, we multiply the image containing the classification errors with the filter mask entry-by-entry resulting in a filtered black-white image of the measuring field.

Although we applied this cleaning postprocessing, we estimated that the error of the classification algorithm is still between 1 and 3%, which is similar to that of human investigator. However, the algorithm always applies the same rule for classification and, unlike humans, therefore always has the same error for all assessments.

Measuring fields

Equal measuring fields were positioned in the inner (iML), intermediate (mML) and outer molecular layer (oML) as well as in the granular (GL) and subgranular layer (sGL) of the DG

and the PC. The PC was chosen as reference area. Each measuring field consisted of three joined rectangular-shaped subfields (200 × 50 pixels) sized 600 × 50 pixels in total, which covered almost the entire suprapyramidal and infrapyramidal blade of the DG. The height of the measuring field was fitted to the GL. All quantifications were carried out for the supra- and infrapyramidal blade of the DG in both hemispheres.

Statistical analysis

According to the functional anatomy of the DG, each lamina gets different afferents (i.e., oML: perforant path fibers, iML/mML: collateral associative fibers (i.e., mossy cells), iML: intrinsic recurrents, sGL: transient connections of new ingrowing cells). Therefore, analysis of variance was used to compare the means of the three different groups for each laminar measuring field separately. For those laminae with significantly different means between the groups, a post hoc test was performed. In case of equal variances of all groups the LSD-test was used, whereas in case of different variances the Tamhane-test was chosen. The statistical analysis of the raw data (Table 2, Supplementary Materials) was performed in SPSS 13. Tables 3 and 4 (Supplementary Material) give an overview of the means and standard error of the means (standard error of mean) of all values from the three groups.

The Neural Network Model

To study whether homeostatic plasticity could account for the observed experimental findings, we created a neural network model of the hippocampal DG in which each cell tries to maintain a target level of electrical activity. A cell can change its activity by adapting its connectivity, i.e., by the formation and deletion of synapses. The network contains N neurons of which the first NE neurons are excitatory and the last N-NE neurons are inhibitory. As in the hippocampus, 90% of the initial neurons are excitatory. Since cells can be added or deleted in our model, N and NE refer to the current number of cells in the network, whereas N^0 and NE^0 indicate the initial total numbers of all cells and of excitatory cells, respectively, which are the same in all simulations (We tested simulations with N^0 = 30, 60, and 100, which had no impact on the qualitative outcomes of the model). As shown in Figure 3, the excitatory cells represent glutamatergic granule and mossy cells, and the inhibitory cells GABAergic basket cells. We initialize the network with nonproliferating cells, i.e., mossy and basket cells, and add granule cells during the simulation (see section *Adding cells*). In other words, NE^0 refers to the number of mossy cells and NE-NE^0 gives the current number of granule cells in the network. Initially, NE equals NE^0. A simple spiking neuron model is used to model neuronal activity.

Each neuron contains A_i presynaptic elements (or axonal elements, representing axonal terminals or varicosities) and D_i postsynaptic elements (or dendritic elements, representing dendritic spines) (Fig. 4a,b) (Wolff and Wagner, 1989; Ziv and Smith, 1996; Fiala et al., 1998; Petrak et al., 2005; Knott et al., 2006; Arellano et al., 2007). Excitatory neurons carry only excitatory presynaptic elements, and inhibitory neurons only inhibitory presynaptic elements. Thus, A_i with $1 \leq i \leq NE$ denotes exclusively excitatory presynaptic elements, and A_i with $NE + 1 \leq i \leq N$ denotes exclusively inhibitory presynaptic elements. Every neuron, regardless of whether it is excitatory or inhibitory (i.e., for $1 \leq i \leq N$), also has D_i^{exc} excitatory and D_i^{inh} inhibitory postsynaptic elements.

Each synapse consists of one presynaptic and one postsynaptic element (an excitatory synapse consists of excitatory pre- and postsynaptic elements, and an inhibitory synapse of inhibitory elements). Pre- and postsynaptic elements can be either free or bound in synapses (Okabe et al., 2001). Of the total number of pre- and postsynaptic elements, A_i, D_i^{exc}, and D_i^{inh} (for $1 \leq i \leq N$), there are a_i, d_i^{exc}, d_i^{inh} free elements, which are available for synapse formation. Synaptic elements, particularly dendritic spines (Trachtenberg et al., 2002; Okamoto et al., 2004; Holtmaat et al., 2005) but also axonal terminals (DePaola et al., 2006), are highly motile structures that are formed or deleted independently of a possible synaptic contact partner. In the beginning of a simulation, neurons are initialized with a set of synapses only (i.e., there are initially no free synaptic elements).

The strength of the synapses is binary, i.e., it has a value of one when a synapse is present and zero when not. Multiple synapses can exist between two neurons. Accordingly, the connection strength $C_{i,j}$ between two neurons is the total number of synapses between neuron j (presynaptic) and i (postsynaptic). As neurons with indices 1 to NE are excitatory and NE+1 to N are inhibitory, the connectivity matrix $\boldsymbol{C}$ [Eq. (1)] can be divided into four clusters of combinations among excitatory and inhibitory cells (The cluster of excitatory cells can be further subdivided into mossy and granule cells.):

$$\boldsymbol{C} = \begin{pmatrix} 0 & \cdots & \boldsymbol{C}_{1,NE} & \boldsymbol{C}_{1,NE+1} & \cdots & \boldsymbol{C}_{1,N} \\ \vdots & \ddots & \vdots & \vdots & \ddots & \vdots \\ \boldsymbol{C}_{NE,1} & \cdots & 0 & \boldsymbol{C}_{NE,NE+1} & \cdots & \boldsymbol{C}_{NE,N} \\ \boldsymbol{C}_{NE+1,1} & \cdots & \boldsymbol{C}_{NE+1,NE} & 0 & \cdots & \boldsymbol{C}_{NE+1,N} \\ \vdots & \ddots & \vdots & \vdots & \ddots & \vdots \\ \boldsymbol{C}_{N,1} & \cdots & \boldsymbol{C}_{N,NE} & \boldsymbol{C}_{N,NE+1} & \cdots & 0 \end{pmatrix} \quad (1)$$

The model has no direct recurrent synapses on the same neurons. Moreover, granule cells do not form synapses onto other granule cells (Fig. 3), just as in the hippocampal DG [not shown in Eq. (3)]. All nonzero entries of the connectivity matrix are positive discrete numbers, including the inhibitory connections [see Eq. (4) how inhibition is treated]. We initialize the network with a random connectivity that is two thirds of the full connectivity: So we distribute $\left\lfloor \frac{2}{3} \cdot N^0 \cdot N^0 \right\rfloor$ synapses on $N^0 \times N^0$ possible combinations among N^0 neurons. As we start the simulation with 30 neurons, we share 600 synapses onto 900 possible combinations of neurons. It is biologically realistic to assume that the network is not fully connected (Stepanyants et al., 2002). Moreover, there is evidence that most

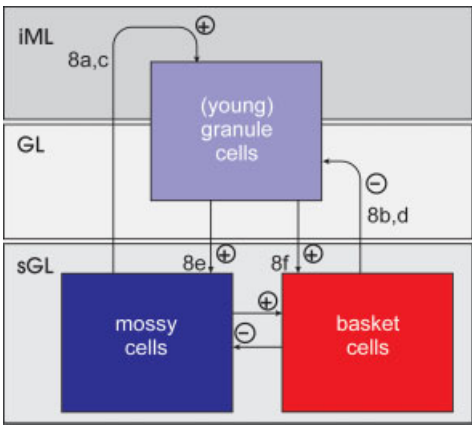

FIGURE 3. Connectivity of the hippocampal DG in the model. The model comprises three different sets of neurons: (1) a growing number of (young) granule cells; (2) mossy cells, providing excitatory input to young granule cells; and (3) basket cells, providing inhibitory input to young granule cells. With respect to the anatomical situation of the hippocampal DG, mossy cells terminate on (young) granule cells within the inner molecular layer (iML). Basket cells predominantly form synapses on cell somata of (young) granule cells in the granule cell layer (GL). (Young) granule cells mainly terminate on mossy and basket cells within the subgranular layer (sGL) and additionally form some recurrent synapses within the iML. The numbers refer to the corresponding figures in the result section. [Color figure can be viewed in the online issue, which is available at www.interscience.wiley.com.]

cortical neurons are connected with each other only by a very few synapses (reviewed in Peters, 2002).

The network connectivity gives rise to a certain level of activity in each neuron. We assume that every neuron adapts its connectivity in order to try to keep its neuronal activity at a certain level. For this homeostatic regulation of activity there is a wealth of experimental data (Wollf and Wager, 1989; Corner and Ramakers, 1992; Turrigiano et al., 1994; Van den Pol et al., 1996; Liu and Kaczmarek, 1998; Turrigiano and Nelson, 2000; Wierenga et al., 2005; Maffei et al., 2006; Turrigiano, 2007). In our model, neurons adapt their connectivity in an activity-dependent manner (Wolff and Wagner, 1983; Devoogd et al., 1985; Lipton and Kater, 1989; Kossel et al., 1995; Sernagor and Grywacz, 1996; Engert and Bonhoeffer, 1999; Kossut and Juliano, 1999; Blaesing et al., 2001; Yuste and Bonhoeffer, 2001; Datwani et al., 2002; Pak and Sheng, 2003; Tian and Copenhagen, 2003; Nägerl et al., 2004; Tailby et al., 2005; reviewed in Fox and Wong, 2005) by adding and deleting pre- and postsynaptic elements, which affect the number of synapses and consequently the connectivity and activity of the cells.

Activity-dependent changes in the number of pre- and postsynaptic elements occur on a longer time scale than the fast changes in neuronal activity (cp. Trachtenberg et al., 2002; DePaola et al., 2006; Toni et al., 2007). In our model, we therefore define two time scales, one for the activity changes of the cell (referred to by t) and a longer time scale for connectivity changes (referred to by T), where the connectivity update $T \rightarrow T + 1$ is done every 1,000 activity time steps. If we assume that spines remodel within a day (Trachtenberg et al., 2002) and, similarly, axonal branches rewire between different postsynaptic targets within one to a very few days (DePaola et al., 2006), we may define that one morphogenetic time step in the model roughly corresponds to 1 day in biological networks.

A simulation consists of iterations through the following six steps:

Calculating neuronal activity

In the model, the probability that a neuron i fires at time $t+1$ depends on its current membrane potential X_i^{t+1} according to a standard sigmoidal firing rate function F_i:

$$F_i^{t+1}(X_i^{t+1}) = \frac{1}{1 + e^{\left(-\frac{X_i^{t+1}-\theta}{\beta}\right)}}, \quad 1 \leq i \leq N, \qquad (2)$$

where θ is the firing threshold and β is the steepness of the threshold function, defining the noise level of neuronal firing.

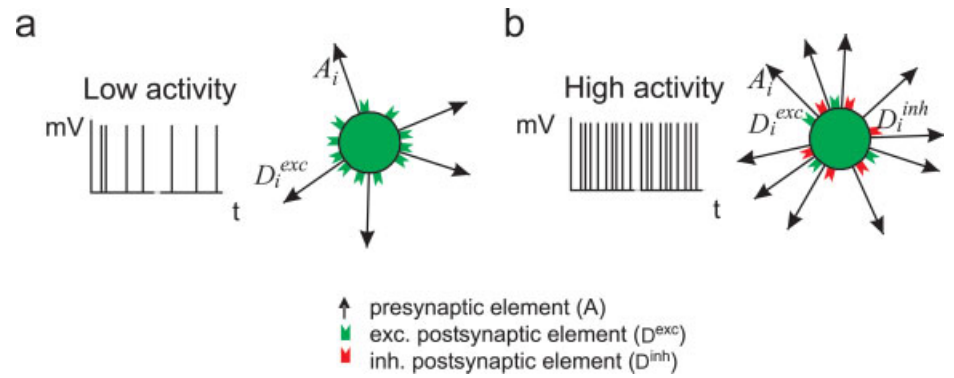

FIGURE 4. Activity-dependent development of synaptic elements in the model. (a) When neuronal firing rates are low, neurons express many excitatory postsynaptic elements in order to increase their chance of getting excitatory inputs. In contrast, the number of presynaptic elements is low when activity is low. (b) If neuronal firing rates are too high, neurons lose excitatory postsynaptic elements, which reduce their excitatory synaptic input. Additionally, there is an increase in the number of inhibitory postsynaptic elements, which increases the likelihood of getting more inhibition. Together, these processes will reduce the activity of the neuron. Further, activity increases the number of presynaptic elements. [Color figure can be viewed in the online issue, which is available at www.interscience.wiley.com.]

The state of each neuron, z_i^t, which is either one or zero, indicates whether neuron i produced a spike at time t. Initially, z_i^0 is randomly set to 1 or 0 so that in average 50% of all neurons are active in the first step. Thereafter ($t > 0$), the firing state of a neuron is determined on the basis of the firing probability F_i. If F_i is greater than a random number r_i drawn from a uniform distribution [0, 1], then the neuron will generate a spike. So the firing state of a neuron at time $t+1$ is given by

$$z_i^{t+1} = \left\{ \begin{array}{ll} 0, & \text{if} \quad F_i^{t+1} < r_i \\ 1, & \text{if} \quad F_i^{t+1} \geq r_i \end{array} \right\}, \quad 1 \leq i \leq N\,. \tag{3}$$

Input from firing excitatory neurons increase, and input from firing inhibitory neurons decrease the membrane potential of a postsynaptic neuron. Thus, the membrane potential of each neuron i is the sum over all its excitatory and inhibitory synaptic inputs:

$$X_i^{t+1} = \sum_{j=1}^{NE} \boldsymbol{C}_{i,j} \cdot z_j^t - \sum_{j=NE+1}^{N} \boldsymbol{C}_{i,j} \cdot z_j^t, \quad 1 \leq i \leq N\,, \tag{4}$$

where $C_{i,j}$ is the number of synapses from neuron j to neuron i.

Adding and deleting pre- and postsynaptic elements (including synapse deletion)

Morphogenetic changes are predominantly mediated by changes in the intracellular concentration of Ca^{2+} (Mattson and Kater, 1987; Kater et al., 1988; Mattson et al., 1988; Kater et al., 1989; Lipton and Kater, 1989; Korkotian and Segal, 2007), which reflect a long-term average of the neuron's firing activity (Ross and Graubard, 1989; Ross, 1989; Li et al., 1996; Liu et al., 1998). At every T, to determine changes in the number of pre- and postsynaptic elements, we therefore take the average s_i^T of the firing probability over the last 1,000 activity time steps t.

We set the desired level of the long-term average of the firing activity for all cells arbitrarily at 0.5. The deviation from this desired level, $\Delta s_i^T = s_i^T - 0.5$, drives the changes in the number of axonal and dendritic elements (Fig. 4). Changes in the number of presynaptic elements (excitatory or inhibitory) are computed by:

$$\Delta A_i = \nu \cdot \Delta s_i \cdot A_i, \quad 1 \leq i \leq N \tag{5}$$

where ν is a velocity term that defines how fast neurons respond to changes in their activity. A small ν results in a slower compensation of the neuronal activity, whereas a large ν makes the compensation faster but may produce overshoot behavior; we take $0 < \nu \ll 1$. On the dendritic site, we have to distinguish between changes in the number of excitatory postsynaptic elements, ΔD_i^{exc}, and changes in the number of inhibitory postsynaptic elements, D_i^{inh}:

$$\Delta D_i^{\text{exc}} = -\nu \cdot \Delta s_i \cdot D_i^{\text{exc}}, \quad 1 \leq i \leq N \tag{6}$$

$$\Delta D_i^{\text{inh}} = \nu \cdot \Delta s_i \cdot D_i^{\text{inh}}, \quad 1 \leq i \leq N \tag{7}$$

Equations (5)–(7) are in agreement with experimental findings showing that an increased average firing rate enhances the number of axonal elements (Fig. 4b) (Merzenich et al., 1984; Mattson, 1988; Lipton and Kater, 1989; Wolff and Wagner, 1989; Wolff and Missler, 1992; Carmichael et al., 2001; Zhong and Wu, 2004; Rekart et al., 2007). With respect to dendritic elements, a neuron reduces excitatory dendritic elements (Kirov and Harris, 1999; Portera-Caillieu, 2003; Kirov et al., 2004) and increases inhibitory dendritic elements (Knott et al., 2002) when its average firing activity becomes too high, while the opposite changes take place when its average firing rate becomes too low (Fig. 4a), which contributes to the homeostasis of neuronal activity of the cell.

Depending on the sign of ΔD_i^{exc}, ΔD_i^{inh} and ΔA_i, pre- and postsynaptic elements are then either added or deleted for each neuron i, $1 \leq i \leq N$. When ΔD_i^{exc}, ΔD_i^{inh} or ΔA_i is negative, we randomly choose $|\Delta D_i^{\text{exc}}|$, $|\Delta D_i^{\text{inh}}|$ or $|\Delta A_i|$ elements (irrespective of whether they are bound in a synapse or not) from the sets of pre- and postsynaptic elements and delete them. When the element chosen is bound in a synapse, the synaptic connection is lost as well, but the pre- or postsynaptic counterpart of the deleted element is kept and available for further synapse formation (see section *Synapse formation*).

After changing the number of pre- and postsynaptic elements, the total number of elements D_i^{exc}, D_i^{inh}, A_i and the number of free elements a_i, d_i^{exc}, d_i^{inh} are updated.

Synapse formation

For synapse formation (Fig. 5a,b), we consider the set of all the a_j free presynaptic elements of all excitatory neurons j, $1 \leq j \leq NE$, and the set of all the d_i^{exc} free excitatory postsynaptic elements of all neurons i, $1 \leq i \leq N$ (i.e., both excitatory and inhibitory neurons). Synapses can in principle be formed between any types of neurons with equal likelihoods; however, model neurons are not allowed to form recurrent synapses to themselves, and granule cells are excluded from forming synaptic contacts among each other. We then fully distribute the smaller set of one type of free elements onto the larger set of the other type. This is done simultaneously. For example, assume that there are more free excitatory presynaptic elements available in the entire network than free excitatory postsynaptic elements. In this case, we select a random subset of the free excitatory presynaptic elements that equals in size the (smaller) set of free excitatory postsynaptic elements. These free excitatory presynaptic elements are then connected to the free excitatory postsynaptic elements. The inverse is done if there are more free excitatory postsynaptic elements available in the

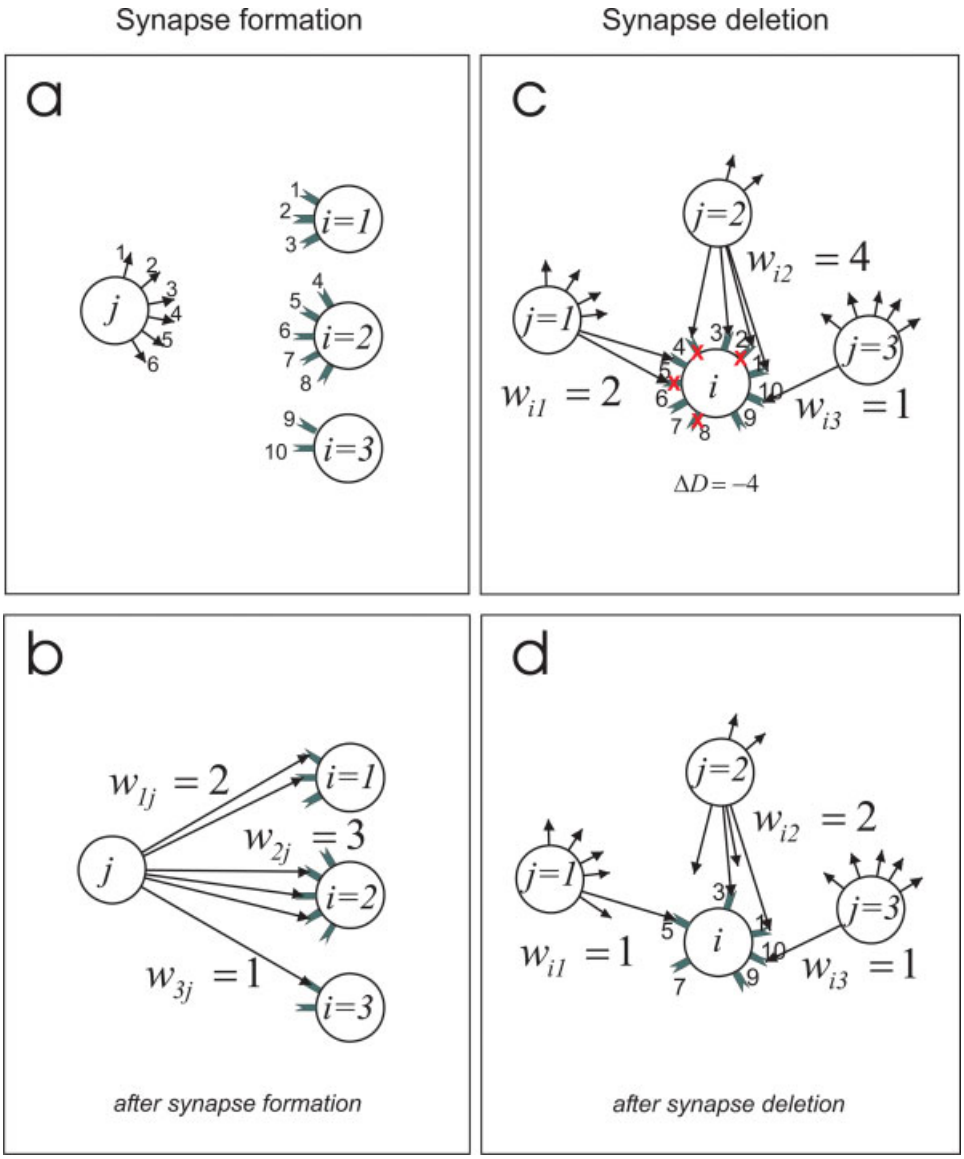

FIGURE 5. Synapse formation and deletion in the model. (a) In the example shown here, there are a total of six presynaptic elements and 10 postsynaptic elements. (b) The minimal number of synaptic elements, in this case the presynaptic elements, are randomly and fully distributed to the postsynaptic elements. This results in proportional synapse formation, whereby neurons with the most postsynaptic elements form the most synapses. In this example, the neuron with five postsynaptic elements gets, by chance, 50% of the presynaptic elements. (c) Another example illustrates that synaptic elements to be deleted are chosen randomly irrespective of whether they are part of a synapse or not. (d) Subsequently, this causes the loss of corresponding synapses. The remaining pre- and postsynaptic elements are again available for further synapse formation. [Color figure can be viewed in the online issue, which is available at www.interscience.wiley.com.]

network than free excitatory presynaptic elements. Thereby, we ensure that recurrent synapses are not formed.

Inhibitory synapses are formed in a separate step. Again, we consider two total sets, one consisting of all the a_j free presynaptic elements of all inhibitory neurons, and one consisting of all the d_i^{inh} free inhibitory postsynaptic elements of all neurons i, $1 \leq i \leq N$ (i.e., both excitatory and inhibitory neurons). The synaptic formation procedure for the inhibitory elements is further the same as that for the excitatory elements.

Subsequently, we update the amount of free synaptic elements a_i, d_i^{exc}, d_i^{inh} of all neurons i, $1 \leq i \leq N$, by the number of synaptic elements that got bound into synapses. Note that the total numbers of synaptic elements A_i, D_i^{exc}, and D_i^{inh} of each neuron do not change by synapse formation.

Cell deletion

Activity-dependent regulation of apoptosis has been proposed by different authors (Gallo et al., 1987; Johnson et al., 1992;

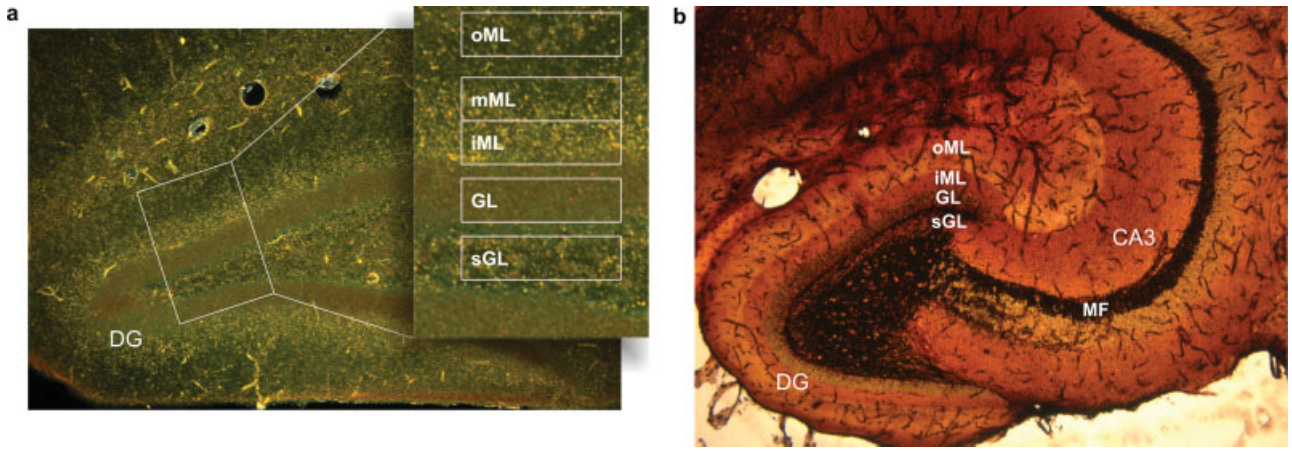

FIGURE 6. Hippocampal DG. The hippocampal layer consists of three separate layers, namely the subgranular layer (sGL), the granule layer (GL) and the molecular layer. The molecular layer is subdivided into the inner molecular layer (iML), the intermediate zone (mML) and the outer molecular layer (oML). (a) Dark field light microscopy image of the hippocampal DG with silver stained LA (Gallyas-technique) appearing as bright granules. Five measuring fields were positioned in the subgranular, granular and molecular layer (as shown by the detailed picture) of both the supra-pyramidal and the infrapyramidal blade of the DG. (b) Bright field image of a TIMM-stained hippocampal slice showing the mossy fiber (MF) bundle projecting from the DG to hilar and hippocampal CA3 regions (black fibers). A dark brown shadow covers the iML in the TIMM staining picture that corresponds well with the layer of highest LA density in the Gallyas-staining picture (see Fig. 6a). [Color figure can be viewed in the online issue, which is available at www.interscience.wiley.com.]

Ono et al., 1997; Ikonomidou et al., 1999; Monti and Contestabile, 2000; Ono et al., 2003). Cell culture studies by Linden (1994) show that the survival of a neuron highly depends on its afferent and efferent support, implying a need for sufficient postsynaptic activity. In the model, we therefore assume that changes in the number of pre- and postsynaptic elements can take place only when the neuron's average activity is not extremely different from its desired value. Only activity values in the range of $0.35 \leq s_i \leq 0.85$ will induce changes in synaptic elements. Outside this range, the cell will undergo apoptosis. (The range is chosen asymmetrical because the algorithm is more vulnerable to inhibition than to excitation.) In each morphogenetic time step T, we check whether a neuron is inside or outside this range. Young neurons get a chance to become imbedded into the network by preventing them from apoptosis for 30 morphogenetic time steps T. In case a neuron is deleted from the network, all synaptic elements of this neuron and consequently all its incoming and outgoing synapses are deleted as well. However, the synaptic elements of the neurons to which the deleted cell was connected remain and can form new synapses in the next synapse formation step. After cell deletion, the numbers of free elements of the remaining neurons are updated. Note that there is no change in their total number of synaptic elements.

Adding new cells

In three different sets of simulations, we add a new excitatory granule cell every 1, 5 or 10 morphogenetic time steps T (CP rates are denoted as CP 1:1, CP 1:5, or CP 1:10). There are no granule cells in the beginning of the simulation, i.e., all granule cells are added during the simulation. We consider CP 1:10 as a moderate CP rate and compare this simulation to control animals with normal CP rates (NRC animals). Both CP 1:5 and CP 1:1 are considered increased proliferation rates. When we add a new cell, we endow it with a certain number of free pre- and postsynaptic elements a_i, d_i^{exc}, d_i^{inh}. Each young granule cell i, $1 \leq i \leq NE$, receives $a_i = \left\lfloor \frac{2}{3} \cdot N^0 \right\rfloor$ free (excitatory) presynaptic elements and $\left\lfloor \frac{2}{3} \cdot N^0 \right\rfloor$ free postsynaptic elements. Of the free postsynaptic elements $d_i^{\text{exc}} = \frac{NE^0}{N^0} \cdot \left\lfloor \frac{2}{3} \cdot N^0 \right\rfloor$ are excitatory and $d_i^{\text{inh}} = \frac{N^0 - NE^0}{N^0} \cdot \left\lfloor \frac{2}{3} \cdot N^0 \right\rfloor$ are inhibitory. The young neurons do not carry any synapses initially.

We also tested simulations with young neurons initially having no synaptic elements at all. In order to obtain similar results, it was necessary to increase the velocity term v, which produced an overshoot in synapse formation and activity, so that young neurons developed axonal elements. In fact, young hippocampal granule cells are more plastic than mature neurons (Schmidt-Hieber et al., 2004). During development neurons show an overshoot in number of synapses that are subsequently pruned by experience to the final adult connectivity (Changeux and Danchin, 1976; Cowan et al., 1984; Kalisman et al., 2005). Assuming that adult dentate neurogenesis resembles ontogeny (Esposito et al., 2005; Laplagne et al., 2007), it is biologically plausible that also young hippocampal neurons show some overshoot behavior.

Updating connectivity

Before we can return to Step 1 (*Calculating neuronal activity*), we need to update the connectivity $C_{i,j}$. First, the number of excitatory cells, NE, and the total number of cells, N, are

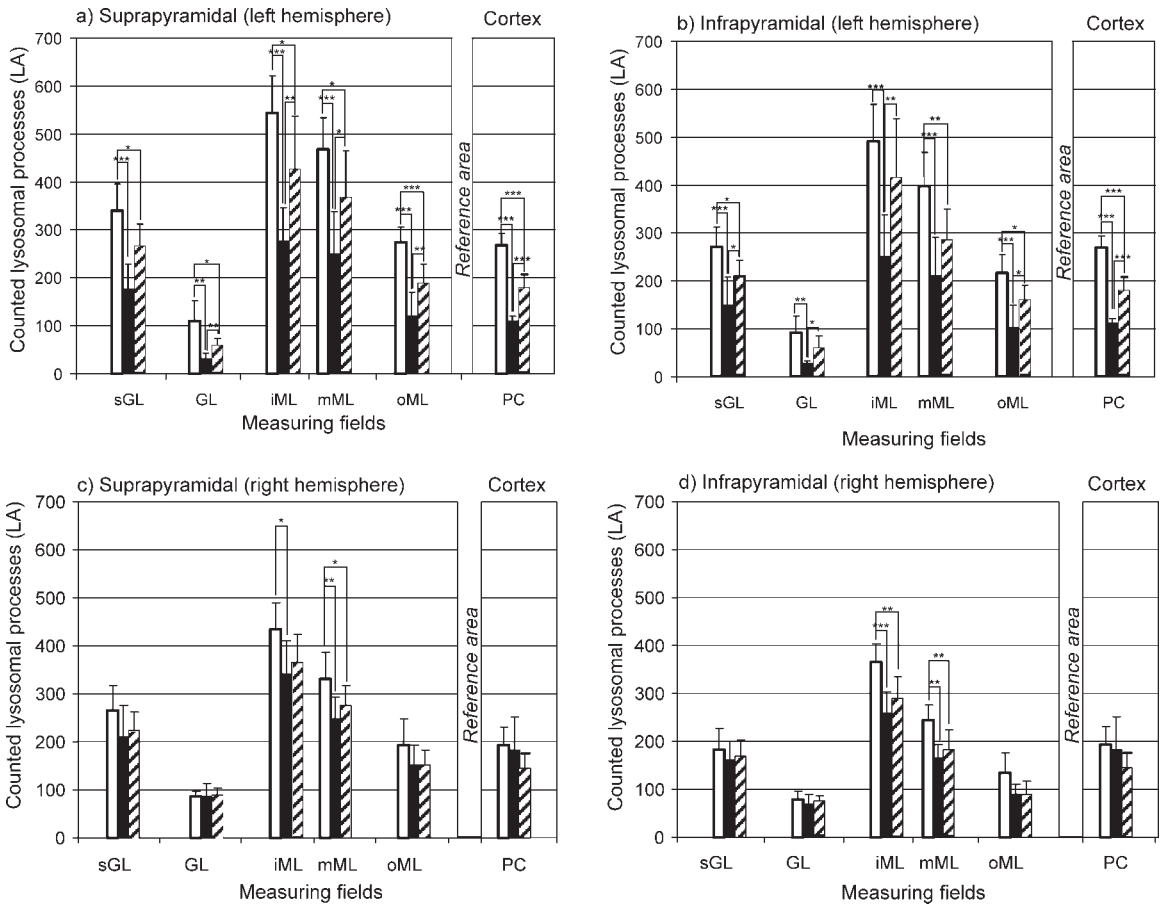

FIGURE 7. Experimental results. Each column shows the average LA distribution in the DG of one of the three groups (white bars: NRC; black bars: IRC; shaded bars: IRC/MA). The IRC group has a reduced LA density compared to the NRC group. LA density of IRC/MA group almost reaches levels of NRC controls again. The effects are most pronounced in the iML and mML, whereas the other layers show a background staining pattern of LA similar to that of the reference area within the parietal cortex. Granule cell layers of both hemispheres and dentate blades across all groups have a very sparse occurrence of LA. (a) Left hemisphere, suprapyramidal blade. (b) Left hemisphere, infrapyramidal blade. (c) Right hemisphere, suprapyramidal blade. (d) Right hemisphere, infrapyramidal blade.

updated according to the number of cells that were added and deleted. Then, for each synapse between neuron j and i that lost either its presynaptic or postsynaptic element, we subtract the total number of synapses, $C_{i,j}$, between these two neurons by one. If more than one synapse is lost between two neurons in one morphogenetic time step, which can happen, $C_{i,j}$ is reduced accordingly. In addition, we set all synapse numbers $C_{i,j}$ to zero when either neuron i or neuron j was deleted. For all neurons j that were able to bind one or more free presynaptic elements to a free postsynaptic element of neuron i, $C_{i,j}$ is increased accordingly.

RESULTS

Experimental Results

Layered occurrence of strong synaptic rewiring in the DG of control animals

In control animals (NRC), we found a band of dense lysosomal accumulation (LAs) (Fig. 6a, Supplementary Table S1) indicating pronounced synaptic rewiring covering the inner molecular layer (iML) in agreement with the layering obtained from TIMM staining (6b). The outer molecular layer (oML) only shows a sparsely scattered background staining of LAs. The subgranular layer (sGL) and also the reference area in the PC have the same distribution pattern of LAs as the oML, together defining a baseline of synaptic reorganisation within the hippocampus and cortex, respectively. This characteristic distribution of LA is present in the supra- and infrapyramidal blade of the DG in both hemispheres.

Animals from isolated rearing have a lowered synaptic rewiring

We quantified the LA densities in the different laminae of the DG from NRC, IRC and IRC/MA animals (Fig. 7, Table 1) in order to study the impact of moderate and increased CP rates on the rewiring of different afferent fibers. In total, the NRC animals show the highest LA in all laminae compared to the other two groups (Supplementary Table S2). In contrast,

TABLE 1.

Average Number of LA in the Different Laminae of the Supra- and Infrapyramidal Blade of the Hippocampal DG

		Superior blade of the DG					Inferior blade of the DG					Cortex
		sGL	GL	iML	mML	oML	sGL	GL	iML	mML	oML	PC
Left hemisphere												
NRC	AVG	339,75	110,88	543,92	467,76	274,73	270,04	89,97	489,80	396,53	214,47	267,36
	σ	56,67	41,30	77,32	66,17	31,16	39,80	34,43	76,41	70,48	38,48	24,79
IRC	AVG	176,08	31,90	275,43	249,56	120,70	147,87	26,52	249,25	208,82	101,67	109,89
	σ	51,59	10,61	70,65	89,52	48,75	58,77	4,96	87,74	81,19	46,96	10,36
IRC/MA	AVG	265,88	59,72	427,97	367,26	188,79	209,29	58,90	413,54	284,22	158,88	179,34
	σ	46,56	14,46	109,00	98,07	39,01	32,22	24,61	123,33	64,17	30,21	27,34
Right hemisphere												
NRC	AVG	265,84	86,19	433,90	329,71	192,18	182,79	78,90	363,86	243,32	132,90	191,63
	σ	51,34	11,16	57,10	56,67	56,98	43,62	16,19	38,91	33,65	41,58	39,25
IRC	AVG	209,21	86,00	339,69	247,42	152,55	161,97	69,73	256,98	164,38	90,18	183,51
	σ	67,55	27,56	70,86	44,06	39,56	37,23	19,91	45,27	27,79	20,08	69,12
IRC/ MA	AVG	224,43	88,67	365,40	276,26	152,08	169,59	76,57	289,86	181,11	90,60	146,04
	σ	35,97	14,82	57,47	39,73	31,96	33,78	10,68	43,62	42,36	26,58	28,49

The laminae are sGL, subgranular layer; GL, granule layer; iML, inner molecular layer; mML, intermediate molecular layer; oML, outer molecular layer; PC, reference area in the parietal cortex. From animals from (semi-) natural rearing conditions (NRC), 8 left hemispheres and 6 right hemispheres were used. From animals from isolated-rearing conditions (IRC), 7 left and 5 right hemispheres were used. Moreover, 7 additional left and 8 additional right hemispheres have been taken from isolated rearing animals after juvenile methamphetamine treatment (IRC/MA).

the IRC group has the lowest LA densities, whereas the LA densities of the IRC/MA group lie in between. The differences between the groups are most significant in those laminae with highest LA densities per se, i.e., the iML and the intermediate molecular layer. Significant results from the group comparisons representative for those laminae with high, medium and low LA densities are summarized as follows.

Pronounced group effects in the inner and intermediate molecular layer

Compared with NRC control animals, the iML (and mML) of the left hemisphere of IRC animals shows an average of LA densities that is significantly reduced (Supplementary Table S3) by 49% (47%) in the suprapyramidal (Fig. 7a) and infrapyramidal blade (Fig. 7b) of the DG. The iML in the IRC/MA group is still reduced by 21% (22%) and 16% (18%) for the suprapyramidal (Fig. 7a) and infrapyramidal blade (Fig. 7b), respectively, which is significant only for the suprapyramidal blade. In the right hemisphere of IRC animals, the LA densities in the iML are significantly reduced by 22% (25%) and 29% (33%) in the suprapyramidal (Fig. 7c) and infrapyramidal blade (Fig. 7d), respectively. LA densities in IRC/MA animals are lowered by only 16% (16%) and 20% (26%), respectively, compared to NRC controls.

Group differences also in hippocampal and cortical background staining

The dentate laminae oML and sGL (Supplementary Table S3) as well as the cortical reference area PC have a similar low LA pattern, which we refer to as background staining. Compared with NRC control animals, in the left hemisphere of IRC group the LA density in the oML (sGL and PC) is significantly reduced by 56% (48 and 59%) in the suprapyramidal (Fig. 7a) and infrapyramidal blade (Fig. 7b) by 56% (45 and 59%), whereas the IRC/MA group is reduced by 31% (22 and 33%) in the suprapyramidal (Fig. 7a) and by 26% (23 and 33%) in the infrapyramidal blade (Fig. 7b). The right hemisphere, in contrast, shows no significant differences with NRC animals (Fig 7c,d).

Reduced LA densities in the granule layer across all groups

Even in the granule layer (GL) (Supplementary Table S3), which is almost free of LA, the maturation effects are still significant, at least in the left hemisphere. Compared with NRC control animals, the left hemisphere of IRC animals show a 72 and 70% reduced LA density in the suprapyramidal (Fig 7a) and infrapyramidal blade (Fig. 7b), respectively, whereas the IRC/MA group is lower by 47 and 34%. In the right hemispheres, there are again no differences with the NRC controls. (Fig. 7c,d)

Lateralization effect

Normal (NRC) and isolated rearing conditions (IRC) entail significant differences in synaptic remodelling in both hemispheres of the adult DG. However, the differences are much more pronounced in the left hemisphere than in the right one (Supplementary Table S4). Interestingly, the methamphetamine

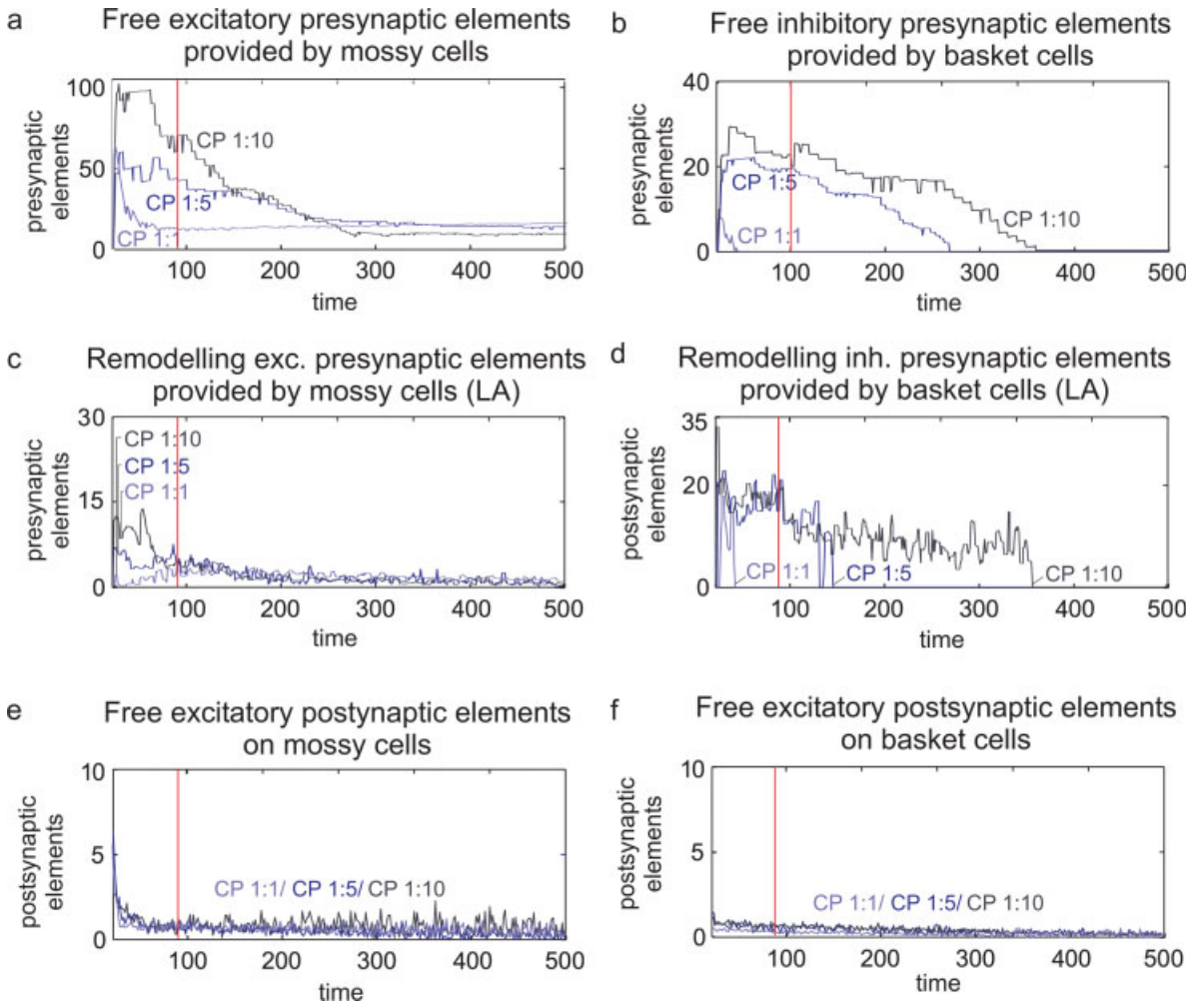

FIGURE 8. Model results. Total number of free synaptic elements over time as dependent on different CP rates. For moderate CP rates, one neuron was added in every 10 morphogenetic time steps (CP 1:10). Increased CP rates add one neuron in every five (CP 1:5) or every single step (CP 1:1). One morphogenetic time step roughly matches 1 day in the development of the animal, and we marked the postnatal day 90 of the animal by a red line in all figures. (a) The total number of free presynaptic elements available for synapse formation offered by the excitatory mossy cells. There is a CP-rate dependent decay of these presynaptic elements over time. (b) The total number of free presynaptic elements offered by the inhibitory basket cells. Only for moderate CP rates is there a high supply of inhibitory presynaptic elements (c) Number of remodelling excitatory presynaptic elements offered by mossy cells. Remodelling presynaptic elements are free elements that arose from the break down of existing synapses (rather than being formed de novo). The number of remodelling presynapses are clearly distinct in the beginning of the simulations, with the highest number for moderate CP rates (CP 1:10) and the lowest for the highest CP rates (CP 1:1). (d) Remodelling inhibitory presynaptic elements offered by basket cells. The numbers are exhausted quickest for highest CP rates. (e) The total number of free excitatory postsynaptic elements on mossy cells. These are targets for excitatory (young) granule cells. (f) The total number of free excitatory postsynaptic elements on inhibitory basket cells. These are also targets for the excitatory granule cells. Interestingly, all the postsynaptic elements that are targets for the young cells do not show a CP-rate dependent decay. [Color figure can be viewed in the online issue, which is available at www.interscience.wiley.com.]

treatment (IRC/MA) again leads to an increased synaptic remodelling which is, however, only significant in the left but not in the right hemisphere. Moreover, the differences are more distinct in the infrapyramidal blade of the right hemisphere, whereas in the left hemisphere the differences are more pronounced in the suprapyramidal blade of the DG.

Modeling Results

In the simulation, ingrowing granule cells compete for pre- and postsynaptic elements of pre-existing excitatory (i.e., mossy cells) and inhibitory neurons (i.e., basket cells) to form synapses (Fig. 3). Free presynaptic (Fig. 8a,b) and postsynaptic elements (Fig. 8e,f) in the simulation are either newly formed or arise from the breakdown of existing synapses (Fig. 8c,d). The time course of the number of free presynaptic elements in the model can be compared with how the supply of excitatory and inhibitory axon terminals develops in the different layers of the DG of the hippocampus (the inner molecular layer, the granular layer, and the subgranular layer). In addition, in the model we can change the CP rate and study how the dynamics of structural plasticity depend on moderate and increased CP rates.

Presynaptic excitatory and inhibitory support for new neurons

Pre-existing excitatory neurons provide a limited number of presynaptic elements that can be used by young neurons to form synapses. Excitatory presynaptic elements provided by the set of nonproliferating cells in the model (i.e., mossy cells) correspond to commissural and associative fibers in the DG, which are mainly provided by excitatory mossy cells (reviewed in Andersen et al., 2006). Inhibitory axon terminals in dentate networks are predominantly provided by GABAergic basket cells, which correspond to inhibitory presynaptic elements in the model. The simulations show a CP rate-dependent decrease in available excitatory (Fig. 8a) and inhibitory presynaptic elements (Fig. 8b) (curve for simulations with moderate CP rates of one new neuron in every 10 time steps, i.e., CP 1:10, compared to CP rates with one new neuron in every five or every single time step, i.e., CP 1:5 or CP 1:1). In the model, the higher the influx of young neurons, the fewer presynaptic elements are available over time. The number of presynaptic elements also decays in simulations with moderate CP rates (CP 1:10).

Remodelling of excitatory and inhibitory presynaptic elements

The free presynaptic elements that arise from synapse deletion are the source for synaptic rewiring in the network (Fig. 8c,d). Both excitatory and inhibitory presynaptic elements remodel and the number of free presynaptic elements that arise from remodelling is in the same way influenced by CP rate as the total amount of free presynaptic elements, meaning that also the number of remodelling presynaptic elements is quicker exhausted when CP rates are high. This particularly holds for inhibitory persynaptic elements (Fig. 8d) and for excitatory presynaptic elements when CP rates are moderately increased (CP 1:5). If CP rates are very high (CP 1:1), there is a small surplus of remodelled synapses in the first third of the simulation run (Fig. 8c) that arises from a compensatory breaking of excitatory synapses in order to counteract raising networks activities because of increasing numbers of excitatory neurons in the network.

Postsynaptic targets for new neurons

Young granule cells extend axons (mossy fibers) to hippocampal CA3 (not modeled), and in addition form collaterals terminating on dentate mossy and basket cells. Figure 8e,f shows the number of free postsynaptic elements available for young granule cells to target their axons on. The number of free postsynaptic elements is much lower than the number of free presynaptic elements. This was also observed in earlier versions of the model (Dammasch et al., 1986; Butz and Teuchert-Noodt, 2006). Interestingly, there is no CP-rate-dependent decrease of free postsynaptic elements for young neurons, neither on excitatory nor on inhibitory neurons. How is this to be explained, considering that presynaptic elements are exhausted with increasing CP rates? The reason for this network behavior lies in the distribution of pre- and postsynaptic elements. If the number of free postsynaptic elements on proliferating cells is smaller than the number of synaptic counterparts, CP rates will determine when this supply for young neurons to form synapses is exhausted. In contrast, if free presynaptic elements on proliferating neurons outnumber postsynaptic elements on nonproliferating neurons already for moderate CP rates, then the reproduction of postsynaptic elements will determine the offer of postsynaptic targets for proliferating cells irrespective of CP rates. In fact, we found that although the rules for pre- and postsynaptic elements are symmetric, all neurons end up with a much larger number of pre- than postsynaptic elements. Thus, formation of input synapses of young neurons is CP rate-dependent in the model, whereas output synapses are not affected by CP rate.

Robustness of the model

The parameter setting influences the quantitative outcome of the simulations but not the qualitative results. In particular, increasing the number of mossy cells in the model raises the level of free presynaptic elements both in the beginning and in the steady state. The same holds for the number of inhibitory basket cells and the final number of free inhibitory presynaptic elements. For high proliferation rates, increasing the number of mossy and basket cells can postpone the time at which steady state is reached or free synaptic elements are exhausted. As long as we keep the number of mossy and basket cells the same across simulations, we obtain the same relationship between synaptic elements and proliferation rate. Changing the firing rates of all neurons or of a particular cell type (e.g., mossy and basket cells), either by additional external input or by lowering the firing thresholds, usually causes temporary morphogenetic changes until all cells have adapted their connectivity so that neuronal activity is restored at set point level. This may postpone the time at which steady state is reached. In contrast, slightly increasing ν, accelerates neuronal compensation, so that the steady state is reached earlier. However, if ν is chosen too large, overshoot behavior may prevent reaching network homeostasis at all, because the network's response to adding new neurons and deleting cells becomes too strong.

DISCUSSION

In our experimental study, we have found an inverse relationship between adult CP and synaptic rewiring in the hippocampal DG. A similar inverse relationship was also obtained in our neuronal network model between CP rate and the number of (remodelling) presynaptic elements. The requirement of homeostasis of neuronal activity in the model gives rise to a reduced synaptic rewiring when CP rates are high.

Synaptic Rewiring in the Experiment and in the Model

As we argued before, ongoing autophagic degradation of synapses by LAs is a fully reversible and functional process within the developing and adult DG. There, it goes along with a

remodelling of axonal terminals rather than a mere loss of synapses. Moreover, during ontogeny it occurs in periods of pronounced synapse formation (Nixdorf, 1986; Nixdorf and Bischof, 1986). As the adult DG with life-long CP and neurogenesis resembles ontogeny (Esposito et al., 2005), we find that in literature on ontogeny (Dawirs et al., 1992; Dawirs et al., 2000; Keller et al., 2000) it is discussed that the amount of LAs is a measure for the current plastic capacity of the dentate network.

In the model, free presynaptic elements indicate the current plastic potential of the network because these are the crucial source for the formation of new synapses. (In fact, both pre- and postsynaptic elements are necessary for synapse formation. However, postsynaptic elements are always available, being subject to homeostatic adaptations of the neurons, whereas presynaptic elements are provided by activity-dependent sprouting and, therefore, determine the amount of new synapses.) Of all free presynaptic elements, we can determine how many come from the break down of synapses, which we consider to correspond to LAs in the layers of the DG.

To describe the process of remodelling axon terminals and dentate network rewiring, we needed a model that distinguishes between pre- and postsynaptic elements. Compared with existing models of neurogenesis, our model is unique in the way it implements synapses and synapse formation, including homeostatic adaptation of connectivity. Existing models investigate the influence of adding and deleting cells on supervised learning (Chambers et al., 2004) or unsupervised learning (Crick and Miranker, 2006). Chambers et al. (2004) show in a three layer network representing the entorhinal cortex, the DG and the CA3 region, that neurogenesis and apoptosis affect pattern storage and retrieval and even memory capacity. Wiskott et al. (2006) found that adding new neurons to artificial neural networks is sufficient to avoid catastrophic interference between sequentially stored patterns. These models represent the synapse as a single element whose strength can be changed by a learning rule. This does not allow the modeling of synaptic rewiring in the sense that one pre- or postsynaptic element is deleted and the remaining one changes its binding partner. In our model, synapse formation is dependent not only on the formation of new synaptic elements but to some extent also on synapse deletion. In existing models, the synapse formation that goes along with adding cells simply arises from increasing the weights that were zero before. This does not describe the morphogenetic process of synaptogenesis as the assembly of pre- and postsynaptic elements. An unexpected outcome of the model is that granule cells in the model form more input than output synapses in the steady state although the rules to form new synapses are the same for incoming and outgoing synapses. This result is interesting as it reflects the anatomical situation in the DG insofar as dentate granule cells receive many incoming synapses but form outgoing synapses with a very small number of target neurons only (reviewed in Andersen et al., 2006).

Synaptic Rewiring and Neurogenesis

Methamphetamine has a late (Hildebrandt, 1999; Hildebrandt et al., 1999; Keller et al., 2000) as well as an acute suppressing effect (Teuchert-Noodt et al., 2000) on CP in isolated-reared gerbils. Although the mechanism by which methamphetamine suppresses CP rates is not fully understood, the IRC/MA group demonstrates that there is an inverse relation between CP rates and synaptic rewiring. Moreover, lateralized differences in synaptic rewiring are significant only for the left hemisphere in which changes in CP rates are significant, too. Although the functional meaning of this lateralization is unknown, it seems to be consistent with findings in schizophrenic brains where changes have been shown in the left temporal lobe (Brown et al., 1986; Crow et al., 1989, Bracha, 1991). Schizophrenic patients show abnormal activity within the left temporal lobe (Mitchell et al., 2001; Rachel et al., 2001).

How can young granule cells influence synaptic rewiring apart from possible transmitter changes that may arise from different rearing conditions and methamphetamine treatment? Recently, two photon-laser imaging studies (Zhao et al., 2006; Laplagne et al., 2006; Toni et al., 2007) have revealed that young dentate granule cells extend postsynaptic filopodia towards adjacent synapses to become occupied by presynaptic axon terminals. It is well known from cell culture studies (reviewed in Purves and Lichtman, 1985) that free postsynaptic receptor plates on developing neurons release neurotrophic factors in order to attract potential presynaptic elements for synapse formation. Although the underlying molecular process cascade is unknown, the breaking of synapses has been demonstrated (Wolff et al., 1989; Grutzendler et al., 2002; Trachtenberg et al., 2002; DePaola et al., 2006; Majewska et al., 2006) and correlates with the morphological development of the postsynaptic spine (Yuste and Bonhoeffer, 2001). Large mushroom spines develop when synapses are potentiated by LTP (Portera-Cailliau et al., 2003; Matsuzaki et al., 2004; Okamoto et al., 2004) and are persistent, whereas thin filopodia-like spines form rather weak synaptic junctions (Holtmaat et al., 2005). Taken together, these experimental findings support that young granule cells might induce synaptic rewiring.

According to our model results, an increased CP rate might be the cause of a reduced plastic capacity of dentate networks for synapse formation and synaptic rewiring. If many young neurons proliferate at the same time, they would, by releasing neurotrophic factors, attract and bind many of the available free presynaptic elements. Moreover, they would induce a strong rewiring of neighboring synapses but quickly exhaust the number of weak synapses, which are the potential source for rewiring (Fig. 9). Since we roughly match the time course of the simulation to the development of the animals, we compare the amount of remodelling presynaptic elements of the different simulations at morphogenetic time step 90 to the number of LA in the animals at postnatal day 90. During an extended middle time period of the simulation, increased CP rates are accompanied by reduced numbers of remodelling presynaptic elements, whereas moderate CP rates go along with the highest presynaptic remodelling. This corresponds to the observed inverse relationship between synaptic rewiring and CP in the animal at postnatal day 90.

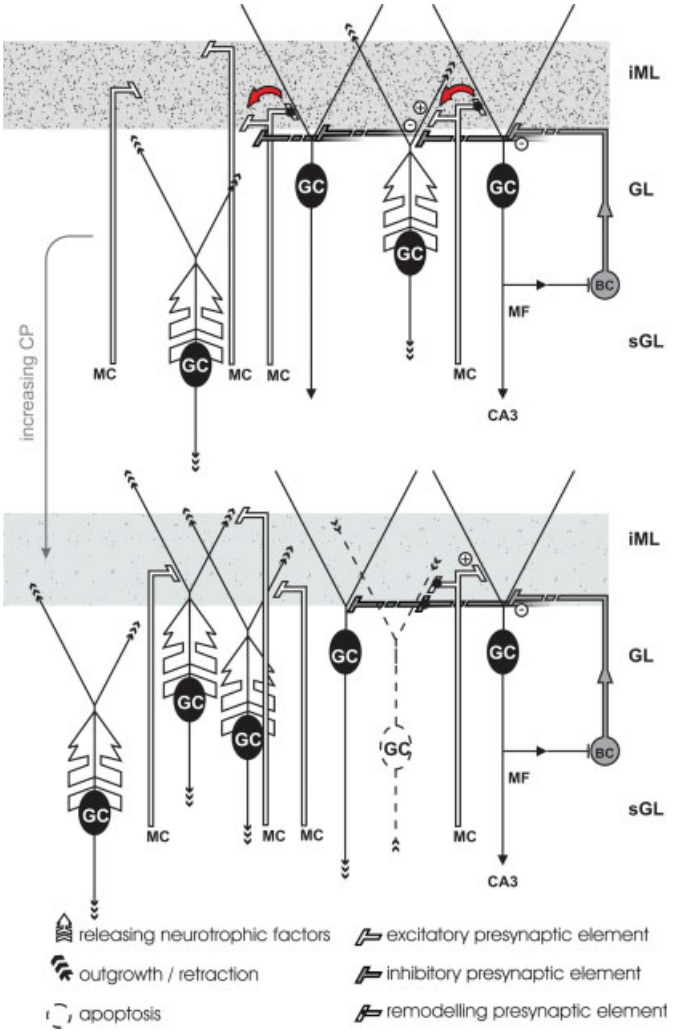

FIGURE 9. Cell proliferation and synaptic rewiring. Young granule cells (GC) migrate from the subgranular layer (sGL) into the granule cell layer (GL), thereby extending dendrites into the molecular layer and axons through the sGL towards the hippocampal CA3 area. The free postsynaptic (i.e., dendritic) elements (not drawn) release neurotrophic factors (white arrows), which attract presynaptic elements of mossy (MC) and basket cells (BC) and may induce lysosomal remodelling of synapses. Black-scattered background indicates LA within the inner molecular layer (iML). If the number of young cells that grow in per unit of time increases, they quickly exhaust the available free presynaptic elements (including those arising from remodelling). This results in a sparse pattern of LA. Cells growing in at later stages will possibly not find enough presynaptic elements to stabilize their neuronal firing at the desired set point level. Any cell that cannot keep its firing rate within a certain range undergoes apoptosis. Presynaptic elements that lost their postsynaptic target by apoptosis remodel and become again available for synapse formation. [Color figure can be viewed in the online issue, which is available at www.nterscience.wiley.com.]

At this point it is necessary to explain that increased proliferation rates in gerbils from isolated rearing do not contradict former studies showing that enriched environment would increase CP rates (cp. Kempermann et al., 1997; Nilsson et al., 1999; Lu et al., 2003; Olson et al., 2006). In fact, we use animals that were housed their whole lives after weaning under either normal or isolated conditions (Winterfeld et al., 1998) and compare their adult baseline conditions of CP. Particularly, gerbils are very vulnerable to isolated rearing and respond with chronically increased CP rates to isolated learning (Hildebrandt, 1999; Keller et al., 2000). This gives rise to a completely different animal model than transferring mice or rats housed in standard laboratory cages to enriched environment at later stages in their development.

Types of Cells and Fibers Involved in Dentate Synaptic Rewiring

The distribution of LA shows a specific pattern across the different dentate laminae (Dawirs et al., 1992; Dawirs et al., 2000). This raises the question as to which nonproliferating cell types and corresponding fibers are predominantly affected by synaptic rewiring.

In the subgranular layer, we would expect that predominantly GABAergic interneurons contribute to the synaptic rewiring, which is in agreement with a recent finding showing that young granule cells initially retrieve excitatory GABAergic input (Ge et al., 2006; 2007a). In contrast, the granule layer that contains the cell bodies of mature granule cells is almost free of LA, which indicates that inhibitory basket cells that form dense plexus around the granule cell somata and the distal apical dendrite are not affected by the rewiring and appear to be stable.

In our study, LAs in the inner molecular layer outnumber by far all other layers. Predominantly, excitatory mossy cells and a minor amount of inhibitory interneurons within the molecular layer form an extended horizontal network of commissural and associative fibers (C/A) terminating on dentate granule cells within the inner molecular layer. We hypothesize that C/A fibers together with septal afferences are the main source of synaptic rewiring within the inner molecular layer. This assumption is backed by former experimental findings that septal afferences (Naumann et al., 1992; Linke et al., 1995; reviewed in Frotscher et al., 1996) and C/A fibers (Lynch et al., 1973; Nadler and Cotman, 1978; Frotscher et al., 1995) show a pronounced reactive capacity to sprout into the outer molecular layer following perforant path lesions (Lynch, 1974; Nadler and Cotman, 1978). The opposite, however, was not found.

The amount of recurrent mossy fibers under physiological conditions terminating in the inner molecular layer is rather low, however, but may increase under pathological conditions like epilepsia (Nadler, 2003; reviewed in Dudek and Sutula, 2007) or after kindling (Lynch and Sutula, 2000). Interestingly, when we allow granule cells to form recurrent synapses in our model, we see that the amount of recurrent synapses is rather low when CP rates are normal. In the model, this effect arises from competition for synapses with pre-existing mossy cells. However, when CP rates are high and there are not enough mossy cells offering presynaptic elements, more granule cells can establish recurrent connections. Thus, it is to be tested

whether a high CP rate might contribute to an increased recurrent circuitry in the hippocampal DG and thereby to epileptogenesis.

In contrast to the inner molecular layer, the outer molecular layer shows a sparse pattern of LA comparable to the background staining in the PC. Besides a few number of GABAergic interneurons, perforant path fibers are the dominating afference terminating on dentate granule cells in the outer molecular layer. These experimental findings may suggest that perforant path fibers do not show a synaptic remodelling but increase their density to occupy young granule cells. In fact, it was shown that the outer molecular layer grows thicker in the adult hippocampus (Duffy and Rakic, 1983; Anthes et al., 1993), whereas the inner molecular layer remains at the same size.

It would be interesting to investigate how dentate CP affects synaptic rewiring in the networks of area CA3 or CA1. From our modeling results we would expect that CP-rate dependent rewiring is restricted to the supply of presynaptic elements for young granule cells but does not affect their postsynaptic targets. Therefore, it would be necessary to complement this work also with experimental data on spine dynamics within the different hippocampal regions.

Possible Functional Role of Synaptic Rewiring in the DG

In general, synaptic rewiring adds a further degree of freedom to neural plasticity (Mel, 2002) and improves memory performance (Chklovskii et al., 2004). Synaptic rewiring in our animal model may be regarded as a functional process (Teuchert-Noodt, 2000), as there is substantial synaptic rewiring in the seminaturally reared control group. What might be the functional role of synaptic rewiring, particularly within the DG? Young granule cells when releasing neurotrophic factors impose a morphogenetic effect on subgranular networks and, later on, on associative networks formed by C/A fibers. This is likely to influence the polysynaptic cascade of inhibition and disinhibition as well as information processing in associative networks, respectively. It has been proposed that neurogenesis may be associated with a clearance of memory traces (Feng et al., 2001). Optimal hippocampal learning and forgetting might be the consequence of a permanent synaptic rewiring associated with neurogenesis. If young granule cells induce synaptic rewiring, then they may already exert functional effects before they are fully synaptically integrated.

However, our work indicates that hippocampal networks may not necessarily benefit from a chronically increased number of young granule cells because it will decrease the capacity of the network to rewire. The consequence might be a worsening of hippocampus related functions. Moreover, we found in a previous modeling study (Butz et al., 2006) that permanently increased CP rates cause a reduced embedding and survival of young granule cells, which is supported by recent experimental literature (Gould et al., 1994; Kitamura and Sugiyama, 2006).

Further modeling studies need to address why neurogenesis and synaptic rewiring are a necessary feature of dentate networks for the encoding of spatial memory but are not required in the storage region (CA3) or the decoding area (CA1).

REFERENCES

Aimone JB, Wiles J, Gage FH. 2006. Potential role for adult neurogenesis in the encoding of time in new memories. Nat Neurosci 9:723–727.

Altman J, Das GD. 1965. Autoradiographic and histological evidence of postnatal hippocampal neurogenesis in rats. J Comp Neurol 124:319–335.

Andersen P, Morris R, Amaral D. 2006. The Hippocampus Book, USA: Oxford University Press Inc.

Anthes DL, LeBoutillier JC, Petit TL. 1993. Structure and plasticity of newly formed adult synapses: A morphometric study in the rat hippocampus. Brain Res 626:50–62.

Arellano JI, Espinosa A, Fairen A, Yuste R, DeFelipe J. 2007. Nonsynaptic dendritic spines in neocortex. Neuroscience 145:464–469.

Becker S. 2005. A computational principle for hippocampal learning and neurogenesis. Hippocampus 15:722–738.

Blaesing B, Nossoll M, Teuchert-Noodt G, Dawirs RR. 2001. Postnatal maturation of prefrontal pyramidal neurones is sensitive to a single early dose of methamphetamine in gerbils (*Meriones unguiculatus*). J Neural Transm 108:101–113.

Bracha HS. 1991. Etiology of structural brain asymmetry in schizophrenia, an alternative hypothesis. Schizophr Bull 17:551–553.

Brown R, Colter N, Corsellis AN, Crow TJ, Firth CD, Tagoe R, Johnstone EC, Marsh L. 1986. Postmortem evidence of structural brain changes in schizophrenia. Arch Gen Psychiatry 43:36–42.

Butz M 2006. Modelling structural plasticity in hippocampal and cortical networks. University of Bielefeld, Germany.

Butz M, Teuchert-Noodt G. 2006. A simulation model for compensatory plasticity in the prefrontal cortex inducing a cortico-cortical dysconnection in early brain development. J Neural Transm 113:695–710.

Butz M, Lehmann K, Dammasch IE, Teuchert-Noodt G. 2006. A theoretical network model to analyse neurogenesis and synaptogenesis in the dentate gyrus. Neural Netw 19:1490–1505.

Cameron HA, Woolley CS, McEwen BS, Gould E. 1993. Differentiation of newly born neurons and glia in the dentate gyrus of the adult rat. Neuroscience 56:337–344.

Carmichael ST, Wei L, Rovainen CM, Woolsey TA. 2001. New patterns of intracortical projections after focal cortical stroke. Neurobiol Dis 8:910–922.

Cecchi GA, Petreanu LT, Alvarez-Buylla A, Magnasco MO. 2001. Unsupervised learning and adaptation in a model of adult neurogenesis. J Comput Neurosci 11:175–182.

Chambers RA, Conroy SK. 2007. Network modeling of adult neurogenesis: Shifting rates of neuronal turnover optimally gears network learning according to novelty gradient. J Cogn Neurosci 19:1–12.

Chambers RA, Potenza MN, Hoffman RE, Miranker W. 2004. Simulated apoptosis/neurogenesis regulates learning and memory capabilities of adaptive neural networks. Neuropsychopharmacology 29:747–758.

Changeux JP, Danchin A. 1976. Selective stabilization of developing synapses as a mechanism for specification of neuronal networks. Nature 264:705–712.

Chechik G, Meilijson I, Ruppin E. 1999. Neuronal regulation: A mechanism for synaptic pruning during brain maturation. Neural Comput 11:2061–2080.

Chklovskii DB, Mel BW, Svoboda K. 2004. Cortical rewiring and information storage. Nature 431:782–788.

Corner MA, Ramakers GJ. 1992. Spontaneous firing as an epigenetic factor in brain development–physiological consequences of chronic tetrodotoxin and picrotoxin exposure on cultured rat neocortex neurons. Brain Res Dev Brain Res 65:57–64.

Cowan WM, Fawcett JW, Oleary DDM, Stanfield BB. 1984. Regressive events in neurogenesis. Science 225:1258–1265.

Crick C, Miranker W. 2006. Apoptosis, neurogenesis, and information content in hebbian networks. Biol Cybern 94:9–19.

Crow TJ, Ball J, Bloom SR, Brown R, Bruton CJ, Colter N, Firth CD, Johnstone EC, Owens DGC, Roberts GW. 1989. Schizophrenia as an anomaly of development of cerebral asymmetry. Arch Gen Psychiatry 46:1145–1150.

Dammasch IE, Wagner GP, Wolff JR. 1986. Self-Stabilization of Neuronal Networks. I. The compensation algorithm for synaptogenesis. Biol Cybern 54:211–222.

Datwani A, Iwasato T, Itohara S, Erzurumlu RS. 2002. NMDA receptor-dependent pattern transfer from afferents to postsynaptic cells and dendritic differentiation in the barrel cortex. Mol Cell Neurosci 21:477–492.

Dawirs RR, Teuchert-Noodt G, Kacza J. 1992. Naturally occurring degrading events in axon terminals of the dentate gyrus and stratum lucidum in the spiny mouse (*Acomys cahirinus*) during maturation, adulthood and aging. Dev Neurosci 14:210–220.

Dawirs RR, Hildebrandt K, Teuchert-Noodt G. 1998. Adult treatment with haloperidol increases dentate granule cell proliferation in the gerbil hippocampus. J Neural Transm 105:317–327.

Dawirs RR, Teuchert-Noodt G, Hildebrandt K, Fei F. 2000. Granule cell proliferation and axon terminal degradation in the dentate gyrus of gerbils (*Meriones unguiculatus*) during maturation, adulthood and aging. J Neural Transm 107:639–647.

DePaola V, Holtmaat A, Knott G, Song S, Wilbrecht L, Caroni P, Svoboda K. 2006. Cell type-specific structural plasticity of axonal branches and boutons in the adult neocortex. Neuron 49:861–875.

Devoogd TJ, Nixdorf B, Nottebohm F. 1985. Synaptogenesis and changes in synaptic morphology related to acquisition of a new behavior. Brain Res 329:304–308.

Dudek FE, Sutula TP. 2007. Epileptogenesis in the dentate gyrus: A critical perspective. Prog Brain Res 163:755–773.

Duffy CJ, Rakic P. 1983. Differentiation of granule cell dendrites in the dentate gyrus of the rhesus monkey: A quantitative golgi study. J Comp Neurol 214:224–237.

Engert F, Bonhoeffer T. 1999. Dendritic spine changes associated with hippocampal long-term synaptic plasticity. Nature 399:66–70.

Eriksson PS, Perfilieva E, Bjork-Eriksson T, Alborn AM, Nordborg C, Peterson DA, Gage FH. 1998. Neurogenesis in the adult human hippocampus. Nat Med 4:1313–1317.

Esposito MS, Piatti VC, Laplagne DA, Morgenstern NA, Ferrari CC, Pitossi FJ, Schinder AF. 2005. Neuronal differentiation in the adult hippocampus recapitulates embryonic development. J Neurosci 25:10074–10086.

Feng R, Rampon C, Tang YP, Shrom D, Jin J, Kyin M, Sopher B, Miller MW, Ware CB, Martin GM, Kim SH, Langdon RB, Sisodia SS, Tsien JZ. 2001. Deficient neurogenesis in forebrain-specific presenilin-1 knockout mice is associated with reduced clearance of hippocampal memory traces. Neuron 32:911–926.

Fiala JC, Feinberg M, Popov V, Harris KM. 1998. Synaptogenesis via dendritic filopodia in developing hippocampal area CA1. J Neurosci 18:8900–8911.

Fox K, Wong RO. 2005. A comparison of experience-dependent plasticity in the visual and somatosensory systems. Neuron 48:465–477.

Frotscher M, Heimrich B, Deller T, Nitsch R. 1995. Understanding the cortex through the hippocampus: Lamina-specific connections of the rat hippocampal neurons. J Anat 187 (Part 3):539–545.

Frotscher M, Deller T, Heimrich B, Forster E, Haas C, Naumann T. 1996. Survival, regeneration and sprouting of central neurons: The rat septohippocampal projection as a model. Ann Anat 178:311–315.

Gallo V, Kingsbury A, Balazs R, Jorgensen OS. 1987. The role of depolarization in the survival and differentiation of cerebellar granule cells in culture. J Neurosci 7:2203–2213.

Gallyas F, Wolff JR, Bottcher H, Zaborszky L. 1980. A reliable and sensitive method to localize terminal degeneration and lysosomes in the central nervous system. Stain Technol 55:299–306.

Gazzaniga MS, Ivry RB, Mangun GR. 2002. Cognitive Neuroscience. New York: Norton.

Ge S, Goh EL, Sailor KA, Kitabatake Y, Ming GL, Song H. 2006. GABA regulates synaptic integration of newly generated neurons in the adult brain. Nature 439:589–593.

Ge S, Pradhan DA, Ming GL, Song H. 2007a. GABA sets the tempo for activity-dependent adult neurogenesis. Trends Neurosci 30:1–8.

Ge S, Yang CH, Hsu KS, Ming GL, Song H. 2007b. A critical period for enhanced synaptic plasticity in newly generated neurons of the adult brain. Neuron 54:559–566.

Gould E, Gross CG. 2002. Neurogenesis in adult mammals: Some progress and problems. J Neurosci 22:619–23.

Gould E, Cameron HA, McEwen BS. 1994. Blockade of NMDA receptors increases cell death and birth in the developing rat dentate gyrus. J Comp Neurol 340:551–565.

Grutzendler J, Kasthuri N, Gan WB. 2002. Long-term dendritic spine stability in the adult cortex. Nature 420:812–816.

Hastings NB, Gould E. 1999. Rapid extension of axons into the CA3 region by adult-generated granule cells. J Comp Neurol 413:146–154.

Hildebrandt K. 1999. Zur modulation neuroplastischer prozesse im hippocampus durch umweltparameter und neuroaktive substanzen: Quantitative analyse zur körnerzellproliferation der adulten maus. Faculty of Biology, University of Bielefeld.

Hildebrandt K, Teuchert-Noodt G, Dawirs RR. 1999. A single neonatal dose of methamphetamine suppresses dentate granule cell proliferation in adult gerbils which is restored to control values by acute doses of haloperidol. J Neural Transm 106:549–558.

Holtmaat AJ, Trachtenberg JT, Wilbrecht L, Shepherd GM, Zhang X, Knott GW, Svoboda K. 2005. Transient and persistent dendritic spines in the neocortex in vivo. Neuron 45:279–291.

Holzgraefe M, Teuchert G, Wolff JR. 1981. Chronic isolation of visual cortex induces reorganization of cortico-cortical connections. In: Flohr H, Precht W, editors. Lesion-induced Neuronal Plasticity in Sensorimotor Systems, Berlin, Heidelberg, New York: Springer-Verlag. pp 351–359.

Ikonomidou C, Bosch F, Miksa M, Bittigau P, Vockler J, Dikranian K, Tenkova TI, Stefovska V, Turski L, Olney JW. 1999. Blockade of NMDA receptors and apoptotic neurodegeneration in the developing brain. Science 283:70–74.

Johnson EM, Jr., Koike T, Franklin J. 1992. A "calcium set-point hypothesis" of neuronal dependence on neurotrophic factor. Exp Neurol 115:163–166.

Kalisman N, Silberberg G, Markram H. 2005. The neocortical microcircuit as a tabula rasa. Proc Natl Acad Sci USA 102:880–885.

Kaplan MS, Bell DH. 1983. Neuronal proliferation in the 9-month-old rodent-radioautographic study of granule cells in the hippocampus. Exp Brain Res 52:1–5.

Kaplan MS, Bell DH. 1984. Mitotic neuroblasts in the 9-day-old and 11-month-old rodent hippocampus. J Neurosci 4:1429–1441.

Kater SB, Mattson MP, Cohan C, Connor J. 1988. Calcium regulation of the neuronal growth cone. Trends Neurosci 11:315–321.

Kater SB, Mattson MP, Guthrie PB. 1989. Calcium-induced neuronal degeneration: A normal growth cone regulating signal gone awry (?). Ann N Y Acad Sci 568:252–261.

Keller A, Bagorda F, Hildebrandt K, Teuchert-Noodt G. 2000. Effects of enriched and of restricted rearing on both neurogenesis and synaptogenesis in the hippocampal dentate gyrus of adult gerbils (*Meriones unguiculatus*). Neurol Psychiatr Brain Res 8:101–107.

Kempermann G, Kuhn HG, Gage FH. 1997. More hippocampal neurons in adult mice living in an enriched environment. Nature 386:493–495.

Kempermann G, Wiskott L, Gage FH. 2004. Functional significance of adult neurogenesis. Curr Opin Neurobiol 14:186–191.

Kirov SA, Harris KM. 1999. Dendrites are more spiny on mature hippocampal neurons when synapses are inactivated. Nat Neurosci 2:878–883.

Kirov SA, Goddard CA, Harris KM. 2004. Age-dependence in the homeostatic upregulation of hippocampal dendritic spine number during blocked synaptic transmission. Neuropharmacology 47:640–648.

Kitamura T, Sugiyama H. 2006. Running wheel exercises accelerate neuronal turnover in mouse dentate gyrus. Neurosci Res 56:45–52.

Knott GW, Quairiaux C, Genoud C, Welker E. 2002. Formation of dendritic spines with GABAergic synapses induced by whisker stimulation in adult mice. Neuron 34:265–273.

Knott GW, Holtmaat A, Wilbrecht L, Welker E, Svoboda K. 2006. Spine growth precedes synapse formation in the adult neocortex in vivo. Nat Neurosci 9:1117–1124.

Korkotian E, Segal M. 2007. Morphological constraints on calcium dependent glutamate receptor trafficking into individual dendritic spine. Cell Calcium 42:41–57.

Kossel A, Lowel S, Bolz J. 1995. Relationships between dendritic fields and functional architecture in striate cortex of normal and visually deprived cats. J Neurosci 15:3913–3926.

Kossut M, Juliano SL. 1999. Anatomical correlates of representational map reorganization induced by partial vibrissectomy in the barrel cortex of adult mice. Neuroscience 92:807–817.

Laplagne DA, Esposito MS, Piatti VC, Morgenstern NA, Zhao C, van Praag H, Gage FH, Schinder AF. 2006. Functional convergence of neurons generated in the developing and adult hippocampus. PLoS Biol 4:e409

Laplagne DA, Kamienkowski JE, Esposito MS, Piatti VC, Zhao C, Gage FH, Schinder AF. 2007. Similar GABAergic inputs in dentate granule cells born during embryonic and adult neurogenesis. Eur J Neurosci 25:2973–2981.

Lehmann K, Butz M, Teuchert-Noodt G. 2005. Offer and demand: Proliferation and survival of neurons in the dentate gyrus. Eur J Neurosci 21:3205–3216.

Leutgeb U. 1986. Plastizität von synaptischen Verbindungen nach Kommissurotomien im Hippocampus der Ratte. Med. Inaugural-Dissertation, Universität Marburg.

Li J, Grynspan F, Berman S, Nixon R, Bursztajn S. 1996. Regional differences in gene expression for calcium activated neutral proteases (calpains) and their endogenous inhibitor calpastatin in mouse brain and spinal cord. J Neurobiol 30:177–191.

Linden R. 1994. The survival of developing neurons: A review of afferent control. Neurosci 58:671–682.

Linke R, Pabst T, Frotscher M. 1995. Development of the hippocamposeptal projection in the rat. J Comp Neurol 351:602–616.

Lipton SA, Kater SB. 1989. Neurotransmitter regulation of neuronal outgrowth, plasticity and survival. Trends Neurosci 12:265–270.

Liu SQ, Kaczmarek LK. 1998. Depolarization selectively increases the expression of the Kv3.1 potassium channel in developing inferior colliculus neurons. J Neurosci 18:8758–8769.

Lu L, Bao G, Chen H, Xia P, Fan X, Zhang J, Pei G, Ma L. 2003. Modification of hippocampal neurogenesis and neuroplasticity by social environments. Exp Neurol 183:600–609.

Lynch GS, Mosko S, Parks T, Cotman CW. 1973. Relocation and hyperdevelopment of the dentate gyrus commissural system after entorhinal lesions in immature rats. Brain Res 50:174–178.

Lynch G. 1974. Functional recovery after lesions of the nervous system. 3. Developmental processes in neural plasticity. The formation of new synaptic connections after brain damage and their possible role in recovery of function Neurosci Res Program Bull 12:228–233.

Lynch M, Sutula T. 2000. Recurrent excitatory connectivity in the dentate gyrus of kindled and kainic acid-treated rats. J Neurophysiol 83:693–704.

Maffei A, Nataraj K, Nelson SB, Turrigiano GG. 2006. Potentiation of cortical inhibition by visual deprivation. Nature 443:81–84.

Majewska AK, Newton JR, Sur M. 2006. Remodeling of synaptic structure in sensory cortical areas in vivo. J Neurosci 26:3021–3029.

Markakis EA, Gage FH. 1999. Adult-generated neurons in the dentate gyrus send axonal projections to field CA3 and are surrounded by synaptic vesicles. J Comp Neurol 406:449–460.

Matsuzaki M, Honkura N, Ellis-Davies GC, Kasai H. 2004. Structural basis of long-term potentiation in single dendritic spines. Nature 429:761–766.

Mattson MP. 1988. Neurotransmitters in the regulation of neuronal cytoarchitecture. Brain Res 472:179–212.

Mattson MP, Kater SB. 1987. Calcium regulation of neurite elongation and growth cone motility. J Neurosci 7:4034–4043.

Mattson MP, Taylor-Hunter A, Kater SB. 1988. Neurite outgrowth in individual neurons of a neuronal population is differentially regulated by calcium and cyclic AMP. J Neurosci 8:1704–1711.

Mel BW. 2002. Have we been hebbing down the wrong path? Neuron 34:175–177.

Meltzer LA, Yabaluri R, Deisseroth K. 2005. A role for circuit homeostasis in adult neurogenesis. Trends Neurosci 28:653–660.

Merzenich MM, Nelson RJ, Stryker MP, Cynader MS, Schoppmann A, Zook JM. 1984. Somatosensory cortical map changes following digit amputation in adult monkeys. J Comp Neurol 224:591–605.

Ming GL, Song H. 2005. Adult neurogenesis in the mammalian central nervous system. Annu Rev Neurosci 28:223–250.

Mitchell RLC, Elliotta R, Woodruff PWR. 2001. fMRI and cognitive dysfunction in schizophrenia. Trends Cog Sci 2:71–81.

Monti B, Contestabile A. 2000. Blockade of the NMDA receptor increases developmental apoptotic elimination of granule neurons and activates caspases in the rat cerebellum. Eur J Neurosci 12:3117–3123.

Nadler JV. 2003. The recurrent mossy fiber pathway of the epileptic brain. Neurochem Res 28:1649–1658.

Nadler JV, Cotman CW. 1978. Interactions between afferents to the dentate gyrus after entorhinal lesion during development: Long-term regulation of choline acetyl-transferase activity. Brain Res 142:174–181.

Naumann T, Linke R, Frotscher M. 1992. Fine structure of rat septohippocampal neurons. I. Identification of septohippocampal projection neurons by retrograde tracing combined with electron microscopic immunocytochemistry and intracellular staining. J Comp Neurol 325:207–218.

Nägerl UV, Eberhorn N, Cambridge SB, Bonhoeffer T. 2004. Bidirectional activity-dependent morphological plasticity in hippocampal neurons. Neuron 44:759–767.

Neddens J, Brandenburg K, Teuchert-Noodt G, Dawirs RR. 2001. Differential environment alters ontogeny of dopamine innervation of the orbital prefrontal cortex in gerbils. J Neurosci Res 63:209–213.

Nilsson M, Perfilieva E, Johansson U, Orwar O, Eriksson PS. 1999. Enriched environment increases neurogenesis in the adult rat dentate gyrus and improves spatial memory. J Neurobiol 39:569–578.

Nixdorf B. 1986. Synaptogenese und Plastizität im rectofugalen System des Zebrafinken. Eine quantitative elektronenmikroskopische Analyse Diss Univ Bielefeld.

Nixdorf B, Bischof HJ. 1986. Postnatal development of synapses in the neuropil of the nucleus rotundus of the cebra finch. A quantitative electron microscopic study. J Comp Neurol 250:133–139.

Okabe S, Miwa A, Okado H. 2001. Spine formation and correlated assembly of presynaptic and postsynaptic molecules. J Neurosci 21:6105–6114.

Okamoto K, Nagai T, Miyawaki A, Hayashi Y. 2004. Rapid and persistent modulation of actin dynamics regulates postsynaptic reor-

ganization underlying bidirectional plasticity. Nat Neurosci 7:1104–1112.
Olson AK, Eadie BD, Ernst C, Christie BR. 2006. Environmental enrichment and voluntary exercise massively increase neurogenesis in the adult hippocampus via dissociable pathways. Hippocampus 16:250–260.
Ono T, Kudo Y, Kohara K, Kawashima S, Ogura A. 1997. Activity-dependent survival of rat cerebellar granule neurons is not associated with sustained elevation of intracellular Ca^{2+}. Neurosci Lett 228:123–126.
Ono T, Sekino-Suzuki N, Kikkawa Y, Yonekawa H, Kawashima S. 2003. Alivin 1, a novel neuronal activity-dependent gene, inhibits apoptosis and promotes survival of cerebellar granule neurons. J Neurosci 23:5887–5896.
Pak DT, Sheng M. 2003. Targeted protein degradation and synapse remodeling by an inducible protein kinase. Science 302:1368–1373.
Peters A. 2002. Examining neocortical circuits: Some background and facts. J Neurocytol 31:183–193.
Petrak LJ, Harris KM, Kirov SA. 2005. Synaptogenesis on mature hippocampal dendrites occurs via filopodia and immature spines during blocked synaptic transmission. J Comp Neurol 484:183–190.
Piatti VC, Esposito MS, Schinder AF. 2006. The timing of neuronal development in adult hippocampal neurogenesis. Neuroscientist 12:463–468.
Portera-Cailliau C, Pan DT, Yuste R. 2003. Activity-regulated dynamic behavior of early dendritic protrusions: Evidence for different types of dendritic filopodia. J Neurosci 23:7129–7142.
Purves D, Lichtman JW. 1985. Principles of Neural Development. Sunderland, MA: Sinauer Ass Inc, pp 433.
Rachel LC, Mitchell RE, Woodruff PWR. 2001. fMRI and cognitive dysfunction in schizophrenia. Trends Cog Sci 2:71–81.
Rekart JL, Sandoval CJ, Routtenberg A. 2007. Learning-induced axonal remodeling: Evolutionary divergence and conservation of two components of the mossy fiber system within Rodentia. Neurobiol Learn Mem 87:225–235.
Rickmann M, Amaral DG, Cowan WM. 1987. Organization of radial glial cells during the development of the rat dentate gyrus. J Comp Neurol 264:449–479.
Ross WN. 1989. Changes in intracellular calcium during neuron activity. Annu Rev Physiol 51:491–506.
Ross WN, Graubard K. 1989. Spatially and temporally resolved calcium concentration changes in oscillating neurons of crab stomatogastric ganglion. Proc Natl Acad Sci USA 86:1679–1683.
Schlessinger AR, Cowan WM, Gottlieb DI. 1975. An autoradiographic study of the time of origin and the pattern of granule cell migration in the dentate gyrus of the rat. J Comp Neurol 159:149–175.
Schmidt-Hieber C, Jonas P, Bischofberger J. 2004. Enhanced synaptic plasticity in newly generated granule cells of the adult hippocampus. Nature 429:184–187.
Seki T, Arai Y. 1993. Highly polysialylated neural cell adhesion molecule (NCAM-H) is expressed by newly generated granule cells in the dentate gyrus of the adult rat. J Neurosci 13:2351–2358.
Sernagor E, Grzywacz NM. 1996. Influence of spontaneous activity and visual experience on developing retinal receptive fields. Curr Biol 6:1503–1508.
Shors TJ, Miesegaes G, Beylin A, Zhao MR, Rydel T, Gould E. 2001. Neurogenesis in the adult is involved in the formation of trace memories. Nature 410:372–376.
Stanfield BB, Trice JE. 1988. Evidence that granule cells generated in the dentate gyrus of adult rats extend axonal projections. Exp Brain Res 72:399–406.
Stepanyants A, Hof PR, Chklovskii DB. 2002. Geometry and structural plasticity of synaptic connectivity. Neuron 34:275–288.
Tailby C, Wright LL, Metha AB, Calford MB. 2005. Activity-dependent maintenance and growth of dendrites in adult cortex. Proc Natl Acad Sci USA 102:4631–4636.
Tashiro A, Makino H, Gage FH. 2007. Experience-specific functional modification of the dentate gyrus through adult neurogenesis: A critical period during an immature stage. J Neurosci 27:3252–3259.
Teuchert-Noodt G. 2000. Neuronal degeneration and reorganization: A mutual principle in pathological and in healthy interactions of limbic and prefrontal circuits. J Neural Transm Suppl 315–333.
Teuchert-Noodt G, Dawirs RR. 1996. Naturally occurring synapse degradation in the developing cerebellum of the mallard (*Anas platyrhynchos*) and the Peking duck (*Forma domestica*). J Hirnforsch 37:547–560.
Teuchert-Noodt G, Breuker KH, Dawirs RR. 1991. Neuronal lysosome accumulation in degrading synapses of sensory-motor and limbic subsystems in the duck *Anas platyrhynchos*: Indication of rearrangements during avian brain development? Dev Neurosci 13:151–163.
Teuchert-Noodt G, Dawirs RR, Hildebrandt K. 2000. Adult treatment with methamphetamine transiently decreases dentate granule cell proliferation in the gerbil hippocampus. J Neural Transm 107:133–143.
Tian N, Copenhagen DR. 2003. Visual stimulation is required for refinement of ON and OFF pathways in postnatal retina. Neuron 39:85–96.
Toni N, Teng EM, Bushong EA, Aimone JB, Zhao C, Consiglio A, van Praag H, Martone ME, Ellisman MH, Gage FH. 2007. Synapse formation on neurons born in the adult hippocampus. Nat Neurosci 10:727–734.
Trachtenberg JT, Chen BE, Knott GW, Feng G, Sanes JR, Welker E, Svoboda K. 2002. Long-term in vivo imaging of experience-dependent synaptic plasticity in adult cortex. Nature 420:788–794.
Turrigiano G. 2007. Homeostatic signaling: The positive side of negative feedback. Curr Opin Neurobiol 17:318–324.
Turrigiano GG, Nelson SB. 2000. Hebb and homeostasis in neuronal plasticity. Curr Opin Neurobiol 10:358–364.
Turrigiano G, Abbott LF, Marder E. 1994. Activity-dependent changes in the intrinsic properties of cultured neurons. Science 264:974–977.
Van den Pol AN, Strecker GJ, Dudek FE. 1996. Excitatory and inhibitory amino acids and synaptic transmission in the suprachiasmatic nucleus. Prog Brain Res 111:41–56.
Van Ooyen A, Van Pelt J. 1994. Activity-dependent outgrowth of neurons and overshoot phenomena in developing neural networks. J Theor Biol 167:27–43.
Van Ooyen A, Van Pelt J, Corner MA. 1995. Implications of activity dependent neurite outgrowth for neuronal morphology and network development. J Theor Biol 172:63–82.
Van Praag H, Kempermann G, Gage FH. 1999. Running increases cell proliferation and neurogenesis in the adult mouse dentate gyrus. Nat Neurosci 2:266–270.
Van Praag H, Schinder AF, Christie BR, Toni N, Palmer TD, Gage FH. 2002. Functional neurogenesis in the adult hippocampus. Nature 415:1030–1034.
Wierenga CJ, Ibata K, Turrigiano GG. 2005. Postsynaptic expression of homeostatic plasticity at neocortical synapses. J Neurosci 25:2895–2905.
Winterfeld KT, Teuchert-Noodt G, Dawirs RR. 1998. Social environment alters both ontogeny of dopamine innervation of the medial prefrontal cortex and maturation of working memory in gerbils (*Meriones unguiculatus*). J Neurosci Res 52:201–209.
Wiskott L, Rasch MJ, Kempermann G. 2006. A functional hypothesis for adult hippocampal neurogenesis: Avoidance of catastrophic interference in the dentate gyrus. Hippocampus 16:329–343.

Wolff JR, Wagner GP. 1983. Selforganization in synaptogenesis: Interaction between the formation of excitatory and inhibitory synapses. In: Basar E, Flohr H, Haken H, Mandell AJ, editors. Synergetics of the Brain, Berlin; Heidelberg; New York; Tokyo: Springer. pp 50–59.

Wolff JR, Missler M. 1992. Synaptic reorganization in developing and adult nervous systems. Ann Anat 174:393–403.

Wolff JR, Leutgeb U, Holzgraefe M, Teuchert G. 1989. Synaptic remodelling during primary and reactive synaptogenesis. In: Rahmann H, editor. Fundamentals of Memory Formation: Neuronal Plasticity and Brain Function, Stuttgart; New York: Gustav Fischer Verlag. pp 68–82.

Yuste R, Bonhoeffer T. 2001. Morphological changes in dendritic spines associated with long-term synaptic plasticity. Annu Rev Neurosci 24:1071–1089.

Zhao C, Teng EM, Summers RG Jr, Ming GL, Gage FH. 2006. Distinct morphological stages of dentate granule neuron maturation in the adult mouse hippocampus. J Neurosci 26:3–11.

Zhong Y, Wu CF. 2004. Neuronal activity and adenylyl cyclase in environment-dependent plasticity of axonal outgrowth in *Drosophila*. J Neurosci 24:1439–1445.

Ziv NE, Smith SJ. 1996. Evidence for a role of dendritic filopodia in synaptogenesis and spine formation. Neuron 17:91–102.